Scalable Monitoring of Tree Canopy Density and Height in India at High Spatial Resolutions

Dhruvi Goyal
Indian Institute of Technology Delhi
Delhi, Delhi, India
dhruvi.goyal@sit.iitd.ac.in

Harsh Singh Chauhan
Indian Institute of Technology Delhi
Delhi, Delhi, India
mcs222052@cse.iitd.ac.in

Aaditeshwar Seth
Indian Institute of Technology Delhi
Delhi, Delhi, India
aseth@cse.iitd.ac.in

Abstract

Monitoring of trees in forests and plantations has become crucial to mitigate the adverse effects of climate change. We present a comprehensive study of building open-source remote sensing-based methods to estimate tree characteristics such as canopy density and tree height at a spatial resolution of 25m, monitored annually, to build indicators for improvement, degradation, afforestation, and deforestation in forests and plantations over time. Our models provide better accuracy compared to existing baseline models. We also provide a detailed analysis of tree changes across almost all the agro-climatic zones in India, over a five-year period (July 2017 - June 2022). The resulting maps and statistical analyses highlight regions that have experienced significant changes, and can assist civil society organizations, government departments, and village-level community institutions to track forests and restoration efforts.

Keywords

forest monitoring, plantation monitoring, remote sensing, machine learning, high-resolution, India, participatory tools

ACM Reference Format:
Dhruvi Goyal, Harsh Singh Chauhan, and Aaditeshwar Seth. 2024. Scalable Monitoring of Tree Canopy Density and Height in India at High Spatial Resolutions. In *The 13th International Conference on Information & Communication Technologies and Development (ICTD 2024), December 09–11, 2024, Nairobi, Kenya.* ACM, New York, NY, USA, 32 pages. https://doi.org/10.1145/3700794.3700798

1 Introduction

Forests play a crucial role in sustaining ecological balances, providing a habitat for diverse species, regulating climate, and supporting human livelihoods [19, 40]. The geographical diversity of India showcases a complex array of eco-regions, such as the Western Ghats, Eastern Himalayas, Sundarbans, and the Thar Desert, each possessing distinct ecological importance and characteristics. Forest health monitoring is essential to ensure that these eco-regions are sustainable [47]. Effective monitoring tools are also vital for implementing Community Forest Rights (CFR) that empower local communities to manage and benefit from forest resources [42, 44]. Historically, official bodies tracked forest changes by conducting manual censuses of forest areas, with countrywide estimates often taking several years to complete. Consequently, there is a pressing need to track and safeguard forests in near real-time to enable timely and appropriate actions. Advanced remote sensing technologies offer a solution, providing continuous and detailed data that can enhance forest conservation and resource management efforts [63].

In addition to forests, small-scale tree plantations outside traditional forest areas are increasingly being recognized for their environmental and economic benefits [10]. Initiatives under the Mahatma Gandhi National Rural Employment Guarantee Act (MGNREGA)[1] and efforts by organizations such as Say Trees in India[2] and TIST in Africa[3], focus on tree planting to improve rural livelihoods. The effectiveness of these initiatives can be improved by monitoring the health of these plantations over time, which can provide insights into their growth, survival rates, and overall impact. The economic benefits include enhanced agro-forestry productivity, increased biodiversity, and potential revenue from sustainably managed plantations. It is essential to have Monitoring, Reporting, and Verification (MRV) tools that can track tree health over time by measuring multiple indicators like tree height variation and canopy cover at a high resolution [21]. This would help in understanding the growth of natural forests and tree-planting activities. Various stakeholders including government officials and Non-Governmental Organizations (NGOs) can also leverage MRV tools for scientific planning to undertake future Afforestation, Reforestation, and Revegetation (ARR) projects [8, 62].

[1]https://nrega.nic.in/
[2]https://www.saytrees.org/
[3]https://program.tist.org/



This work is licensed under a Creative Commons Attribution International 4.0 License.

ICTD 2024, December 09–11, 2024, Nairobi, Kenya
© 2024 Copyright held by the owner/author(s).
ACM ISBN 979-8-4007-1041-4/24/12
https://doi.org/10.1145/3700794.3700798

Furthermore, the global focus on carbon credits has highlighted the importance of tree health monitoring in carbon sequestration efforts [55]. Carbon credits are market-based mechanisms to reduce greenhouse gas emissions, and trees play a significant role in absorbing carbon dioxide from the atmosphere [45, 46]. The MRV systems are crucial for validating carbon sequestration projects, to ensure that the claimed carbon reductions are accurate and credible [61]. ARR projects can generate carbon credits to get financial incentives for furthering tree planting and forest restoration efforts. Robust tree health monitoring ensures the success of these projects, thereby contributing to climate change mitigation and sustainable development.

To effectively manage these nature-based solutions, the integration of remote sensing technologies with participatory methods has also emerged as a powerful approach [3, 6, 7, 35]. There is a need for open-source, reliable, cost-effective, and user-friendly participatory tools that could assist marginalized communities, village representatives, NGOs, and government officials to plan and monitor plantation sites in a better way. Such monitoring tools can also be used by communities to generate evidence to show tree plantation growth over time and to bargain more effectively with carbon auditing and monitoring agencies [51].

Towards meeting these goals, our research focuses on developing and utilizing remote sensing-based methods to track tree sites' health over time, specifically by analyzing changes in tree cover land-use land-cover (LULC), canopy density, and canopy height estimates. The processes of afforestation (the growth of new trees on lands that previously did not have trees) and deforestation (the removal of trees and conversion of forested areas to non-forested lands) are critical indicators of forest health. Furthermore, within tree cover regions, tracking finer changes like improvements (increase in canopy density and tree height) and degradation (reduction in canopy density and tree height) can assists in understanding more detailed changes.

Researchers have used different types of in-situ data collection and high resolution remote sensing products to estimate tree characteristics such as its diameter at breast height, canopy height, and density, which are then used to monitor the tree's health as well as measure above-ground biomass or carbon stock using the allometric equations [39, 55, 58]. This is done by using ground measurements to calibrate Airborne LiDAR Satellite (ALS) data in the study area [28, 33, 50] or fitting a regression model to estimate in-situ forest inventory measurements using optical data at a coarse resolution [12, 13, 23, 26, 59]. These methods are expensive, only confined to a specific area of interest, and cannot be generalized to a larger area (country or global level). The Global Ecosystem Dynamics Investigation (GEDI) project [11] is an open-source space-borne LiDAR mission that provides data about 3-dimensional tree characteristics. This data can serve as ground truth to estimate the tree Canopy Height (CH) and Canopy Cover Density (CCD) at varied resolutions using frequently available optical and Synthetic Aperture Radar (SAR) data [54]. Our work utilizes GEDI data as ground truth and builds open-source remote sensing models that can provide timely and efficient monitoring of tree health at a fine scale of 25m to support informed decision-making and sustainable management practices over the years.

To be able to provide a generic solution in India's diverse climatic and soil conditions, we build an Agro-Climatic Zone (ACZ)-specific models using high-resolution open-source satellite data to estimate CCD and CH at 25m spatial resolutions and generate outputs of the overall tree health changes pan-India. ACZ-wise models aim to capture the local uniqueness of each region and improve performance compared to a single generalized model for the entire country. Our research aims at building methods that can track degradation and improvement along with deforestation and afforestation at granular resolution across India, ensuring a finer understanding of tree conditions. In the future, we plan to plug these outputs into open-source participatory tools that can enable local communities, NGOs, or government departments to easily track tree health changes in their region of interest. A flowchart representing an overview of the entire methodological pipeline at the agro-climatic zone (ACZ) level is shown in Figure 1. For each ACZ, the open-source Sentinel-1 and Sentinel-2 satellite data are gathered and processed for tree cover plots for which GEDI data is available. A machine learning model is trained and fine-tuned to obtain the best canopy density and canopy height distribution classifiers. The CCD and CH models can be combined to assess overall tree cover health in a particular year and the changes that happened across years in a given area. Our main contributions are the following:

- We build spatiotemporally robust models to estimate tree canopy height distribution and canopy cover density at 25m x 25m spatial resolutions.
- We generate output maps for the canopy density, canopy height, and overall tree health indicators in a particular year.
- We track the year-on-year and long-term tree health changes, and provide interpretable categories for easier exposition.
- We conduct in-depth tree health change analysis from agricultural year (AY)[4] July 2017 to AY 2021 for all the ACZ across India, and discuss our findings.

[4]In India, agricultural year (AY) is considered from July to June, and has 3 seasons (Kharif, Rabi and Zaid) based on agriculture and monsoon patterns, which is explained in detail in Section 3.1

All outputs, including the code and model, are available openly at https://github.com/Dhruvi-Goyal/Tree-Health-Monitoring.

The rest of the paper is structured as follows: Section 2 highlights existing literature in this domain. Section 3 outlines the detailed methodology of tree CCD and CH distribution modeling, followed by its performance evaluation in Section 4. The tree health change categorization is described in Section 5, along with a comparison with existing baseline techniques. Section 6 lays down the change maps and detailed analysis across India. Finally, Section 7 concludes with the key findings and future directions for this work.

2 Literature Review

This section reviews the existing remote sensing-based tree health monitoring methods in detail in Section 2.1. We also discuss in Section 2.2 some existing participatory applications that use remote sensing outputs.

2.1 Remote-Sensing Based Methods

Monitoring forest change using satellite data is actively used to get frequent updates on forest activities [3, 6, 7, 35]. Different methods exist in the literature to track forest changes and can be categorized along two axes, whether they operate at a pixel-level or image-level, and whether they do a direct change detection or infer change by differencing cross-sectional outputs at different timestamps.

Pixel-level change detection methods analyze time-series data (satellite bands or derived vegetation indices) for each pixel, to identify significant changes and pinpoint moments when a sudden alteration in land cover occurs. Pratihast et al. [9] demonstrated a method to use the Breaks for Additive Season and Trend (BFAST) algorithm at pixel-level Landsat data to detect breakpoints in time series to identify changes happening in the forest areas. BFAST requires the specification of a historical or baseline period and a monitoring period for which changes need to be mapped. Ghaderpour et al. [16] proposed a Just Upon Spectrum and Trend (JUST) method to detect forest changes. This method uses Landsat-8 satellite imagery to get NDVI[5] values and has the potential to detect changes in forest cover with unequally spaced observations. These methods effectively capture temporal patterns, enabling them to detect gradual or abrupt changes over time, but as we show later, they are sensitive to noise and missing data.

Pixel-level cross-sectional change detection method involves building a model to estimate tree characteristics at different time points (generally annual) and then detect changes happening in the forests by comparing the tree health outputs at distinct time points. The forest health at a particular time is computed by analyzing individual pixel's spectral bands and derived vegetation indices, and using thresholding or Machine Learning (ML) based methods. Eskandari et al. built a regression model to predict canopy cover marked via Google Earth Pro and field surveys, using only the computed NDVI from Sentinel-2 [13]. The thresholding method is computationally efficient and easy to understand, which also serves as a baseline for multiple studies to compare their model's performance. However, it does not capture complex relationships and is susceptible to atmospheric variations. Geremew et al. trained two support vector regressors to predict CCD and CH (RH98) obtained from GEDI using the top 20 features derived from several satellite sources, including Advanced Land Observing Satellite - Phased Array type L-band Synthetic Aperture Radar (ALOS-PALSAR), Landsat-8, and Shuttle Radar Topography Mission (SRTM)'s Digital Elevation Model (DEM) product [15]. Wang et al. trained a Catboost model to estimate tree cover in the Eastern Himalayas using Moderate Resolution Imaging Spectroradiometer (MODIS) MOD44B, Landsat spectral bands, and the Climate Research Unit's temperature and precipitation data [60]. They also leveraged the Bi-temporal class probabilities model to classify forest changes into 4 different classes, viz., forest gain without loss, forest loss without gain, forest gain after loss, and forest loss after gain. Potapov, *et al.* trained an ensemble regression tree-based model using GEDI data to predict maximum canopy height at a 30 m resolution and generated a global map for 2019 [49]. They further displayed the canopy height changes from 2000 to 2020 on their Google Earth Engine application. Multiple other works have fit classic ML models to estimate tree characteristics obtained from GEDI, field surveys, or aerial vehicles, using diverse satellite datasets, including Sentinel-1&2, Landsat, ALOS-PALSAR, SRTM DEM, and Visible Infrared Imaging Radiometer Suite (VIIRS) [14, 17, 18, 23, 25, 28, 38, 48, 52, 53, 59]. All these models are trained on data confined to a specific region across the world.

Image-level change detection methods involve training a Convolutional Neural Network (CNN) or transfer learning models for image analysis to classify or segment images and detect the changes directly. These methods are primarily being utilized to detect deforestation and afforestation rather than finer changes in CH or CCD. Rockwell, *et al.* [41] used Landsat satellite imagery to train a deep-learning model to detect deforestation. They trained a two input CNN with the Residual Networks (ResNet) transfer learning model architecture on different agro-climatic zones across the globe. State-of-the-art methods like Siamese networks can identify deforestation or afforestation changes with higher accuracy [1], but detecting forest degradation or improvement over time is a challenging problem as it requires granular

[5]Normalized Difference Vegetation Index (NDVI) is used to identify the amount of greenness in a region. It is explained in detail in Table 1

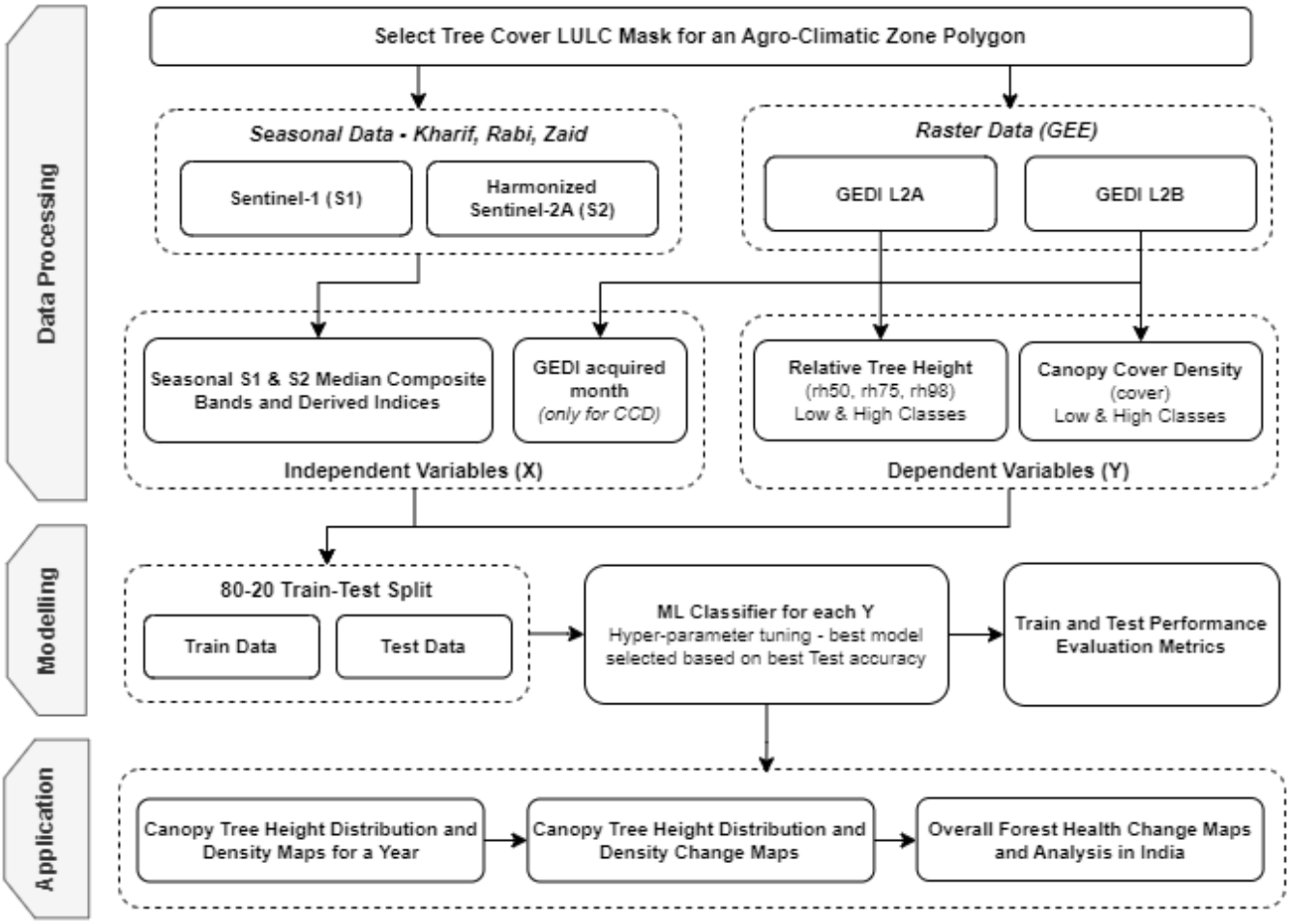


Figure 1: Overview of the Proposed Tree Health Monitoring Pipeline

groundtruth data of changes that have happened with tree canopy height and canopy cover density.

Image-level cross-sectional change detection methods involve training a CNN-based architecture to obtain tree characteristics for a single satellite image taken at a time and then compare it across different time points to get change maps. The World Resources Institute (WRI) [4] has built a tree mapping tool to detect tree characteristics outside dense forest regions at a 10m resolution. Research has also proposed a probabilistic deep neural network with ensemble CNNs to estimate GEDI's relative height metrics using Sentinel-2 optical images to address potential underestimation of smaller canopies [27]. Another work by Liu, *et al.* interpolated canopy height data obtained from Drones and GEDI for a few areas to obtain predictions for all of China using nearest neighbor deep neural networks and tests on GEDI data [29]. This approach does not scale to other years for which GEDI data is unavailable. All these methods have a large computational footprint that involves millions of parameters to be trained at the image level and hence requires substantial resources and extensive training data for achieving optimal parameter tuning.

Most of the existing models are calibrated using data from outside India, and the ones that are done in an Indian setting are limited to a specific small regions and have not been tested for temporal robustness across years. In India, the Forest Survey of India (FSI) measures forest inventories for sample plots from different forest types, and extends the estimation using Linear Imaging and Self Scanning Sensor (LISS III) satellite data, to release reports every two years [43]. The latest Forest Survey Report 2021 provides the data collected in 2019 on forest health, canopy cover, carbon stocks, and forest fires, as well as highlights state-wise changes compared to previous assessments. However, the raw data collected by FSI and plot-level tree characteristics estimates are publicly unavailable. This highlights the need to develop open-source

Indian tree site-specific state-of-the-art health monitoring models. Additionally, most of the existing work focuses only on predicting maximum tree canopy height within a plot which can fail to capture deterioration, for example, if the tallest trees remain intact but other trees are degraded in a plot. Hence, there is a need to consider CH distribution while doing change analysis, rather than just maximum or median tree CH. Additionally, no researchers to the best of our knowledge have combined CCD and CH distribution together to represent overall forest health with a set of easily interpretable categories for users. This is where our contribution lies.

2.2 Participatory Tools

Most of the remote-sensing models discussed in Section 2.1 need to be made more easily accessible through participatory tools, so that communities can use them to monitor and manage forests and plantations, or official bodies can utilize them to decide critical areas where ARR activities need to be conducted. A few such forest and plantation health monitoring tools developed by research organizations are available for public use. Global Forest Watch (GFW)[6] is a near real-time forest activity monitoring tool developed by WRI along with its partners, to track year-wise changes in forest cover, deforestation rates, and tree cover loss from the year 2000 onward using remote sensing data. The 3 Sided Cube organization worked with GFW partners to build a mobile application called Forest Watcher[7] that enables forest communities or officials to track forest changes offline in up to 20,000 sq. km. areas of interest. Global Land Analysis and Discovery (GLAD)[8] is a tool developed by the University of Maryland that uses statistical techniques on optical and SAR data to provide near real-time deforestation or forest degradation alerts. It however does not differentiate between deforestation and degradation of the trees. These publicly available global tools provide useful indicators but do not provide recent afforestation or improvements information, as well as do not consider canopy height distribution within a tree plot to track changes.

Along similar lines, Taking Root[9] built a tool named FARM-TRACE (Taking Root's Technology Platform), which is used by the standards body Plan-Vivo, to assist farmers to check the health of their trees by providing the location, tree characteristics, and species information [2]. This tool is used to estimate biomass, carbon sequestration, and other information in tropical regions. It is a semi-automated tool, where the people must feed in a few mandatory tree-related information so that a machine learning model can be trained to make the predictions more accurate. Another participatory application called MyTree[10] developed by the i-Tree Cooperative also takes inputs from the user about their trees and provides information about carbon dioxide and air pollution removal.

Similar to many of these applications, we plan to distribute our outputs through the Commons Connect Android application to assist communities, governments, or NGOs, to track tree health within and outside forests and undertake appropriate management and new ARR initiatives [34].

3 Methodology

Plantation growth differs across agro-climatic zones (ACZs) because of diverse local environmental factors, and therefore we learn separate models for each ACZ. Figure 2 shows the ACZ map of India along with their zone number mapping. The following sub-sections explain the data processing and modeling pipeline shown in Figure 1.

3.1 Data Acquisition

Our work utilizes the datasets available on the open Google Earth Engine (GEE) platform[11]. GEE hosts different datasets in raster and vector formats, as well as provides functionalities for efficiently merging and processing large datasets. The canopy cover density and relative tree heights obtained from GEDI datasets were considered the ground truth and were used as the dependent output variable for modeling. Seasonal median composite values of bands and derived vegetation indices of Sentinel-1 and Sentinel-2 were used as the independent input features for modeling. India has three main seasons for agriculture: the Kharif (July - October) season during the monsoons, the Rabi (November - February) post-monsoon season, and the Zaid (March - June) summer season in an Agriculture Year (AY). Trees are found to also follow a similar cycle and adjust to the monsoon water availability, and hence we train our models on data segregated on AYs. The details about the exact datasets acquired and pre-processed for modeling are mentioned below.

3.1.1 GEDI. The rasterized version of GEDI L2A and GEDI L2B datasets were obtained from GEE, for getting the canopy height distribution and canopy cover density respectively. GEDI is a space-borne LiDAR mission by NASA which measures and provides a 3-dimensional tree canopy structures at a 25m spatial resolution [11]. The GEDI instrument emits laser pulses and measures the time it takes for the pulses to return after hitting the tree canopy and ground, which

[6] https://www.globalforestwatch.org/map/
[7] https://forestwatcher.globalforestwatch.org/
[8] https://glad.earthengine.app/
[9] https://takingroot.com/
[10] https://mytree.itreetools.org/
[11] https://earthengine.google.com/

leads to quantifying the tree's structural data above the ground. Multiple filters are applied to the canopy height distribution data from GEDI L2A product during retrieval to obtain good quality samples for modelling[12]. Similarly, a few filters are also applied to canopy density data while retrieving the "cover" band value from the GEDI L2B product[13].

Although we can train models for all tens of percentile values of tree height to get the entire canopy height distribution, but since it will be very difficult to interpret as well as resource intensive to compute, hence we chose to model only the statistical representative median, 75th percentile, and maximum relative tree height values. Research has shown that GEDI's 98th percentile tree height value of the plot is a good representative for maximum tree height on-ground in the Indian context [17]. Hence, the rh98 value is taken instead of rh100 in the current setting, for the maximum tree height estimation.

The timestamp at which GEDI data was obtained was also used as a feature, to account for seasonal changes in the canopy. A cyclic transformation was applied to the month number so that December (month 12) of a given AY is adjacent to January (month 1) of the same AY[14]. This enabled us to train the CCD model to predict month-wise canopy cover output for a year as CCD changes across the seasons for deciduous trees. The month feature was not used in the CH modeling as CH does not change noticeably across months.

GEDI data is available from 25th March 2019 to 1st March 2023, which contains 3 complete Agriculture Years (AYs), from July 2019 - June 2022 (AY 2019, 2020, 2021). Therefore, AY 2019 and 2020 data samples were divided into 80% train and 20% test sets after data balancing (explained in subsection 3.2, and samples from AY 2021 were used as out-of-sample data points for evaluation and comparison with existing baseline methods. The evaluation on AY 2021 data also highlights the temporal robustness of the models.

3.1.2 Sentinel-1. This is a C-band Synthetic Aperture Radar (SAR) instrument designed by the European Space Agency (ESA) which uses microwave radar waves to create images of the Earth's surface [57]. The C-band radar waves can penetrate clouds and capture above-ground land variations, allowing for continuous data collection regardless of weather conditions or the time of day. Our work requires estimation of canopy height and canopy cover density of trees, which are all above-ground, and hence the C-band SAR data acts as a good choice. We utilized seasonal median composite of Vertical-Vertical (VV) and Vertical-Horizontal (VH) polarisation bands data obtained using Interferometric Wide Swath (IW) instrument mode, which captures canopy characteristics. The data was resampled at 25m resolution to match the GEDI data. The different vegetation indices derived from VV and VH bands, used in this study are provided in Table 1.

3.1.3 Sentinel-2. This is a part of ESA's Copernicus program and consists of a pair of optical imaging satellites. These satellites capture high-resolution, multispectral images across 13 bands, ranging from visible to multiple infrared bands [30]. Optical data sources capture reflected sunlight to generate images, which are then used to analyze various features of the Earth's surface including vegetation health. We use the harmonized Top of Atmosphere (TOA) data (Sentinel-2A) that is hosted on the GEE platform and corrected for atmospheric radiations. The TOA data represents surface reflectance values measured by satellite sensors at the top of the Earth's atmosphere. GEE hosts the harmonized TOA version that standardizes the TOA measurements across different satellite passes. The median composite values for the bands B1, B2, B3, B4, B5, B6, B7, B8, B11, and B12 were obtained from the data which had less than 1% cloud cover. These bands are available at different resolutions, ranging from 10 m to 60 m, and were resampled to 25m to match GEDI's resolution. Table 1 lists down all the vegetation indices derived from the Sentinel-2 bands which are used for tree cover health modeling in this work.

3.1.4 Auxiliary Data. The Dynamic World [5] and ESA World Cover [64] Land Use Land Cover (LULC) data's *trees* class are used to filter tree cover pixels on which the model is trained. These LULC maps are available at a 10m resolution and hence are reprojected to 25m resolution to match the GEDI resolution. They are laid over GEDI pixels and only the points that belong to the trees class in both the LULC data sources are considered for modeling. As ESA World Cover data does not exist for all the years when Sentinel-1&2 data are available, therefore it is just used for training purposes to ensure good quality data for modeling. Only the Dynamic World cover mask is used to obtain the tree cover pixels for analysis purposes and monitoring tree health in subsequent AYs.

[12]**Filters on GEDI L2A:** Quality Flag = 1, Degrade Flag = 0, Sensitivity ≥ 0.98, Number of Detected Modes != 0, rh25 ≥ 0 (to remove those points which have wrongly calibrated ground elevation and canopy height metrics), Absolute deviation between GEDI's DEM and SRTM's DEM should be no more than 75

[13]**Filters on GEDI L2B:** Quality Flag = 1, Degrade Flag = 0, Sensitivity ≥ 0.98

[14]A standard method used to perform cyclic transformations to **month** (1-12) feature is to derive 2-encoded features, by applying sine [$\sin(2\pi * month)$] and cosine [$\cos(2\pi * month)$] transformations that scale month values between [-1, 1]. As the sine and cosine are cyclic functions, they make month 1 adjacent to month 12 in an AY

Satellite	Derived Index	Formula	Significance
Sentinel-1	VV-VH Ratio	$\frac{VV}{VH}$	Enhances the distinction between different vegetation types by comparing polarization responses
	VH-VV Ratio	$\frac{VH}{VV}$	Emphasizes the backscatter differences related to vegetation structure
	SAR Normalized Difference Vegetation Index (SAR-NDVI)	$\frac{VH - VV}{VH + VV}$	Highlights vegetation by reducing soil background effects, providing clearer vegetation signals in radar imagery
	Difference Vegetation Index (DVI)	$VH - VV$	Captures the absolute difference in backscatter between two bands, useful for distinguishing dense vegetation
	Sum Vegetation Index (SVI)	$VH + VV$	Aggregates radar backscatter information to enhance overall vegetation signal strength
	Relative Difference Vegetation Index (RDVI)	$\frac{VH}{VV} - \frac{VV}{VH}$	Measures relative backscatter differences to emphasize vegetation structure variations
	Normalized Relative Difference Vegetation Index (NRDVI)	$\frac{\frac{VH}{VV} - \frac{VV}{VH}}{\frac{VH}{VV} + \frac{VV}{VH}}$	Normalizes relative backscatter differences to enhance the detection of vegetation changes
	Sum of Squared Difference Vegetation Index (SSDVI)	$VH^2 - VV^2$	Magnifies vegetation-related signals by emphasizing the variance between radar bands
Sentinel-2	Normalized Difference Vegetation Index (NDVI)	$\frac{NIR - Red}{NIR + Red}$	Widely-used indicator of vegetation health and greenness, correlating strongly with canopy density, but saturates at high density.
	Normalized Difference Water Index (NDWI)	$\frac{NIR - SWIR2}{NIR + SWIR2}$	Enhances vegetation moisture content analysis, indirectly reflecting tree health and vigor
	Enhanced Vegetation Index (EVI)	$2.5 * \frac{NIR - Red}{NIR + 6 * Red - 7.5 * Blue + 1}$	Reduces atmospheric interference for more accurate measurements of dense vegetation
	Optimized Soil-Adjusted Vegetation Index (OSAVI)	$\frac{NIR - Red}{NIR + Red + 0.16}$	Adjusts for soil brightness, improving estimates in areas with sparse vegetation cover
	Atmospherically Resistant Vegetation Index (ARVI)	$\frac{NIR - 2 * Red + Blue}{NIR + 2 * Red + Blue}$	Mitigates atmospheric scattering effects, providing more reliable canopy health in hazy conditions
	Visible Atmospherically Resistant Index (VARI)	$\frac{Green - Red}{Green + Red - Blue}$	Specifically designed for visible spectrum data, enhancing tree health estimates under variable atmospheric conditions

Table 1: Derived Indices from Sentinel-1 and Sentinel-2 Bands

3.2 Modelling

For each ACZ, four separate models are trained, to predict (1) the canopy cover density, and (2) the median, (3) 75th percentile, and (4) maximum tree heights as the 98th percentile, for 25m resolution tree plots in a given AY. We found that continuous value predictions were not very reliable and hence we trained binary classifiers. For each of the four tasks, the binary classes are specified as low or high. If the value for a sample is greater than the median value for that ACZ then the sample is labeled as high, and low otherwise. We first isolated the GEDI groundtruth for each ACZ, computed the median value thresholds for CCD, median CH, 75th percentile CH, and maximum CH, and labeled the sample as high or low for the respective machine learning task, i.e. the output Y label for the prediction task. Since each ACZ has different sets of typical tree species and climatic conditions, hence different thresholds are obtained for the low and high classes for each ACZ. For example, the Eastern Himalayan Region mostly consists of temperate broadleaf & evergreen forests, and hence has a higher CCD threshold of (86%), as compared to the Middle Gangetic Plains Region that primarily comprises tropical dry deciduous forests and has a lower CCD threshold (50%). Figure 3 shows the median thresholds considered for CCD and CH bands across different ACZs.

We did not build models for the West Coast Plains and Hills Region (zone 12), Gujarat Plains and Hills Region (zone 13), Western Dry Region (zone 14), and Islands Region (zone 15) due to insufficient GEDI data for these areas.

We verified our choice of using the median values as thresholds for the low and high classes by also training models for other thresholds and observed which models gave the least difference between train and test sets, to avoid over-fitting. The median threshold was found to be the right choice.

As explained earlier, seasonal median composite Sentinel-1 and Sentinel-2 bands & derived indices act as the set of features (input X values for the prediction task). Cyclic monthly values were also used as features for the CCD model. Multiple ML classifiers (Random Forest, Decision Trees, LightGBM, XGBoost, Support Vector Machine) were then evaluated to estimate the tree characteristics (Y). The XGBoost model was found to provide the best performance with the least over-fitting on the training set, and hence was chosen after hyperparameter tuning for each of the cases to classify the data into low or high classes.

The raw canopy height distribution classes do not give an easy-to-understand explanation of tree canopy height variation in a plot. Table 2 shows a conversion of the median, 75th percentile, and maximum tree canopy height classes into comprehensible classes that can be explained easily to potential users of the output. An overall tree height class is assigned based on the distribution of different tree height classes. In the first two cases where at least 75% of the trees are of low height, the overall tree height class is stated as consisting of mostly short trees. Similarly, in the last two cases where more than half of the trees have high tree heights, the overall tree height class is stated as consisting of mostly tall trees. Finally, the rest of the cases have most of the trees with mixed heights and hence are stated as medium-height trees. The medium-height trees can be further distinguished based on the low or high spread of heights in the trees, but that level of detailed classification is restricted in this work, to keep it easily understandable by communities.

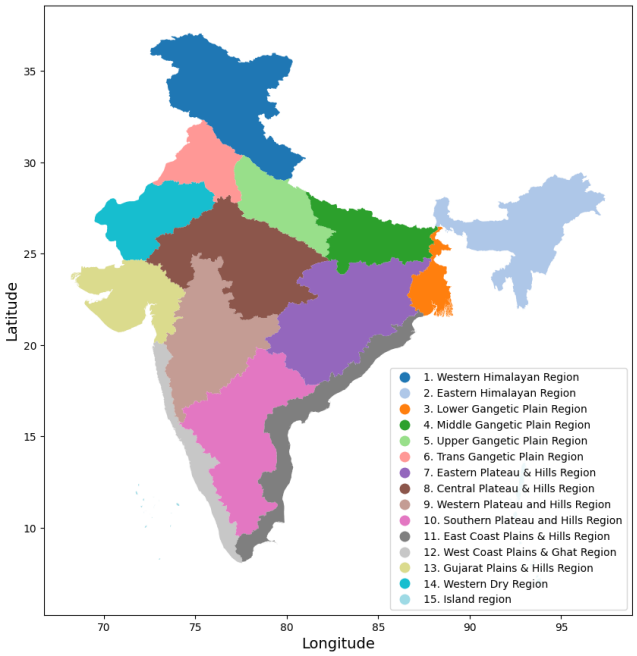


Figure 2: The map of modeled ACZ with their corresponding zone numbers

4 Results

This section discusses the results obtained on East Coast Plains and Hills Region (ECPAHR) in detail and later summarizes the overall performance observed on all the ACZ. The paper shows the model's performance on the train-test datasets, followed by evaluating it on other years. It also correlates the seasonal variation observed for the CCD for an ACZ with the actual on-ground tree species variations observed for that ACZ. Additionally, the model's output stability analysis across years is studied and a correction mechanism is designed. Lastly, the comparison between the developed model's results with the existing baseline methods is also discussed in this section.

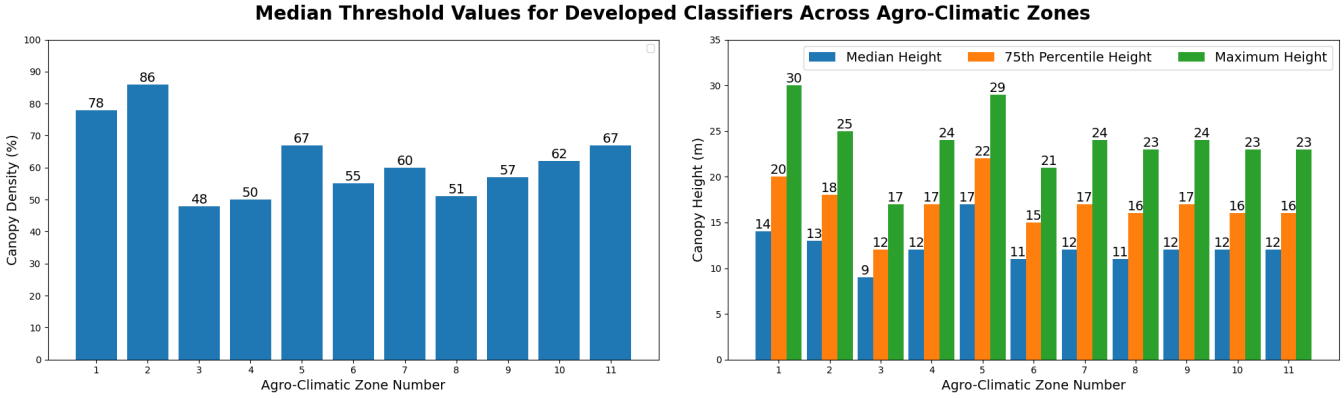


Figure 3: Thresholds used for Classifying CCD and Relative CH Data into Low/High Classes Across Different ACZ

Median Height	75th Percentile Height	Maximum Height	Overall Height Class
Low	Low	Low	Short Trees
Low	Low	High	Short Trees
Low	High	Low	Medium Height Trees
Low	High	High	Medium Height Trees
High	Low	Low	Medium Height Trees
High	Low	High	Medium Height Trees
High	High	Low	Tall Trees
High	High	High	Tall Trees

Table 2: Codifying the canopy height class based on the median, 75th percentile, and maximum tree canopy height class values

4.1 Performance of Models on Train-Test Data

The performance evaluation metrics for classification - accuracy, precision, recall, and F1 score - are computed for all the four XGBoost models, to predict CCD and relative heights of CH (median, 75th percentile, and maximum tree heights), at 25m resolution. Table 3 summarizes the results obtained on 80% train and 20% test sets by all the models across AY 2019 and 2020, for ECPAHR. The thresholds used to classify data into low and high classes were 67% for CCD, 12m for median CH, 16m for 75th percentile CH, and 23m for maximum CH. The macro F1 score is used as the primary metric for evaluation as it averages out the F1 score obtained individually on both the classes, and weighs each class equally, irrespective of the number of samples in each class.

4.2 Temporal Robustness of Models

The performance of all the developed models is further evaluated on the next year's data, i.e., unseen AY 2021 (July 2021 - June 2022) GEDI data. This is temporally out of the sample dataset, as no data points from this year were used for training the model. Hence, this method helps to investigate the temporal robustness of the models across years. Table 3 summarizes the models' performance evaluation metrics on the AY 2021 data points. The results for AY 2021 show a slight deterioration from the test accuracy of 2-6% for the various tree health models, which we believe is tolerable, and

Model	Train Data				Test Data				AY 2021			
	A	P	R	F1	A	P	R	F1	A	P	R	F1
Canopy Cover Density	81	81	81	81	73	73	73	73	69	69	70	69
Median Tree Height	78	78	78	78	69	69	69	69	64	66	63	62
75th Percentile Tree Height	76	76	76	76	69	69	69	69	63	66	62	60
Maximum Tree Height	75	75	75	75	69	69	69	69	67	67	65	64

Table 3: Performance of Canopy Cover Density and Different Canopy Height Classifiers on Train, Test, and Out of Sample Data. (A: Accuracy; P: Precision; R: Recall; F1: F1-Score)

the overall accuracy our models are able to achieve is better than the state of the art. This facilitates using our developed models for predicting tree health indicators in the future for an AY, whenever new Sentinel-1 and Sentinel-2 composites are available for that AY.

4.3 Stability Analysis of the Model Outputs

The models' predictions across consecutive years must be stable and non-fluctuating, i.e. a sudden flip in let's say CCD as (Low - Low - High - Low - Low) across consecutive years would be very odd. This may happen due to incorrect model outputs that could arise from spurious satellite sensor errors or missing data. We consider CCD outputs for the same month in each year (December for ECPAHR, for which the accuracy was highest, also likely because of this period being relatively cloud free) and hence expect that the outputs across consecutive years should be monotonically increasing or decreasing and should not have such fluctuations. Similarly, instability in the outputs for CH models or LULC tree cover predictions would be odd. Overall, we found that both CCD and CH models showed <1% of such odd fluctuations across AY 2016 to AY 2022 in ECPAHR. Therefore, it seems that the the models are largely stable across the years.

However, we still build rules to correct such fluctuations whenever we can do so with high confidence. We do not correct cases where we may be less confident that such fluctuations could actually be correct. Since the outputs are computed from AY 2016 to AY 2022, we buid a set of 5-year fluctuation correction rules that are applied on AY 2018 (using the 2016-2020 window), and similarly on AY 2019 (using the 2017-2021 window) and AY 2020 (using the 2018-2022 window); and 4-year correction rules are applied on the left edge AY 2017 (using the 2016-2019) window and on the right edge AY 2021 (using the 2019-2022 window). Additionally, there is also missing data due to occasional unavailability of Sentinel-1&2 in a few years in a few locations (due to spurious satellite sensor issues and high cloud cover in a few areas) which prevents our models from producing an output for some pixels. Such cases arising from missing data can also be filled using this method (E.g.: if we encounter Low - Low - Missing Data - Low - Low outputs then the missing data can be filled as Low in Year 3). Following are regex-like rules to correct fluctuations in the outputs across years, with high confidence:

Consider "V" as the CCD/CH model's output value of a particular class (high/low), and "?" can take any output value (high/low) or can be missing.

For the 5-year window:

- For the V-V-[X=?]-V-V pattern, **'X'** is set to **'V'** with **high confidence**
- For the V-!V-[X=?]-?-? (or) V-?-[X=?]-!V-? (or) V-?-[X=?]-?-!V (or) ?-V-[X=?]-!V-? (or) ?-V-[X=?]-?-!V (or) ?-?-[X=?]-V-!V patterns, **'X'** is left **unchanged** but marked as **low confidence**

For the 4-year window:

- For the V-[X=?]-V-V (or) V-V-[X=?]-V patterns, **'X'** is set to **'V'** with **high confidence**
- For the V-[X=?]-!V-? (or) V-[X=?]-?-!V (or) ?-[X=?]-V-!V (or) V-!V-[X=?]-? (or) V-?-[X=?]-!V (or) ?-V-[X=?]-!V patterns, **'X'** is **unchanged** but marked as **low confidence**

Since we cannot get any preceding information about fluctuations seen in AY 2016 or succeeding information about fluctuations seen in AY 2022, since they are edge years, all the outputs are considered as **low confidence** for these years. In subsequent years, once AY 2023 tree health outputs are computed then AY 2021 and AY 2022 outputs can be re-calibrated for any fluctuations.

The same approach is also adopted to correct tree cover LULC outputs (E.g. if there are Trees - Trees - No Trees - Trees - Trees in a consecutive 5-year period, then *No Trees* is changed to *Trees* in Year 3).

Confidence scores assigned to various years are further used for change analysis and to assign confidence values to the tree health change outputs. This is explained later in Section 5.5.

4.4 Comparison with Existing Baseline Methods

4.4.1 Comparison with NDVI Based Baseline Models. Several research works have only used NDVI derived from optical data like Sentinel-2 or Landsat satellite bands and predicted tree characteristics by thresholding the NDVI values [13]. Due to its popularity, we use this as a baseline method to compare against our models. A boxplot was generated for seasonal NDVI values for low and high classes of GEDI-based tree canopy density and height values. A threshold that gave the best accuracy on distinguishing the classes for each band on the GEDI July 2019 - June 2021 data was selected. An NDVI threshold of 0.578 for the Rabi season gave the best separation, compared to the Zaid season's NDVI threshold of 0.4. Figure 4 shows the performance (macro-F1 score) comparison between the NDVI-based thresholding done during the Rabi season and our models for canopy density and height distribution on AY 2021 data for all the ACZ. It can be seen that our XGBoost-based models are significantly better than the NDVI-based baseline method in most of the ACZs. The highest difference in performance between our models and the NDVI-based baseline method is observed in the Upper Gangetic Plain Region (ACZ 5) for CH distribution, and Western Plateau and Hills Region (ACZ 9) for CCD. Additionally, it is also observed that the NDVI-based method had low individual class precision and recall values, which wasn't the case with our classifiers.

4.4.2 Comparison with GLAD Outputs. GLAD gives maximum canopy height estimates at a global scale, for the years 2000, 2005, 2015, and 2020. Their model was developed using GEDI data and Landsat satellite images at a 30m resolution [49]. They used GEDI's RH95 band as the proxy for the maximum canopy height across the world. The common period when both GLAD and our model's results were available is 2020. GLAD provides estimates based on calendar year and our model provides predictions for agricultural year. Therefore, our and GLAD's maximum canopy height prediction models were evaluated on GEDI's July 2020 - December 2020 data points for all the considered ACZ in this study. Furthermore, GLAD does not give predictions in non-forest areas (which had high tree cover loss from 2000 to 2020, or where no trees were ≥3m canopy height). Hence, all such points where GLAD's CH estimates were not available for 2020, were filtered out and were not considered for the evaluation. The average root mean squared error (RMSE) of GLAD predictions on the GEDI dataset across all ACZ is 12.6m. Furthermore, the maximum CH values of GLAD were also classified into low and high classes, based on the thresholds computed for each ACZ. Figure 5 shows a comparison of the F1 score obtained by GLAD and our models across different ACZs. The average F1 score of GLAD is 45.5%, which is on average 33% worse than our developed models. Therefore, we observe that our maximum canopy height models perform better in an Indian setting than the global GLAD-based models. The potential reason behind this is that GLAD models were originally trained using datasets from outside India and such global models may be unable to capture local variations well. This emphasizes that having an ACZ-specific model captures the local context and gives better results.

4.5 Performance Evaluation of all the Agro-Climatic Zones' Models

The models for all 11 ACZs were trained using the same methodology and performance evaluation strategy as discussed in the previous sections. The F1 score on AY 2021 data ranged from 58% for the Eastern Himalayan region to 76% for the Middle Gangetic Plains region for the CCD models. For CH distribution, the F1 score on AY 2021 varied between 56% to 74% for maximum CH, 57% to 75% for 75th percentile CH, and 58% to 75% for median CH. The average performance on AY 2021 across all the ACZ in India is 67.2% for CCD, 64.9% for maximum CH, 64.2% for 75th percentile CH, and 64% for median CH. The results presented in this section are raw model results, before correcting the temporal output fluctuations. The outputs after rectifying these fluctuations are expected to further enhance the results somewhat. This shows the current models are spatio-temporally robust to predict tree cover health indicators.

5 Tree Cover Health Change Categorization

With the primary goal of monitoring the health of trees to analyze changes happening to the tree characteristics over time, we next discuss the method we have built to classify changes in tree cover across the years. First, a site is assessed for any afforestation or deforestation based on the tree cover LULC mask, and if the tree cover remains intact, then the site is assessed for degradation or improvement based on changes in the CCD and CH distribution. All the change analysis is done after temporally correcting the outputs for any fluctuations across years, as mentioned in Section 4.3. The modal values of the current, previous, and next year outputs for a year are considered as the final health output for that year and are considered for detecting change

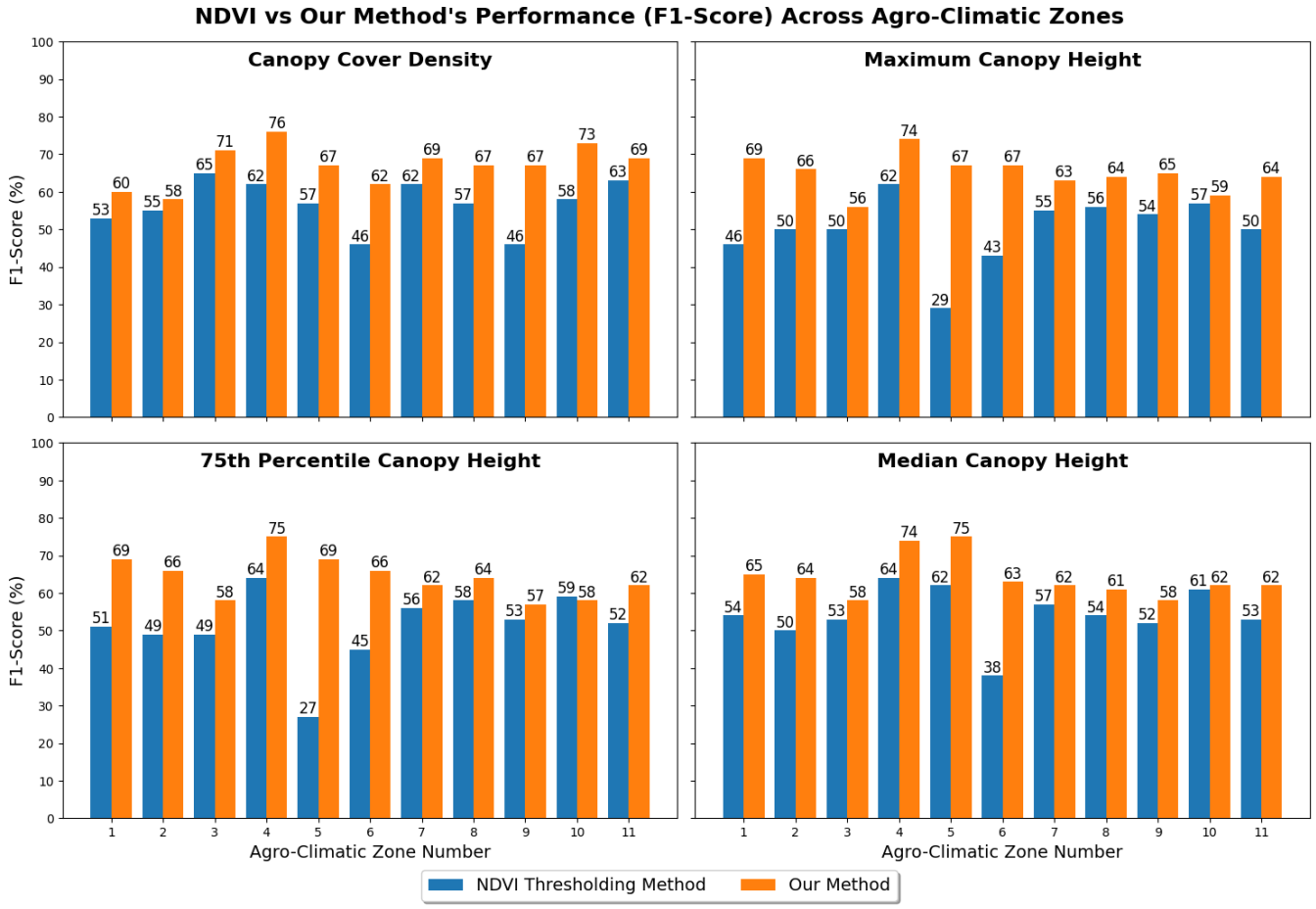


Figure 4: NDVI v/s our Models Performance Comparison Across Different ACZ on AY 2021 Data

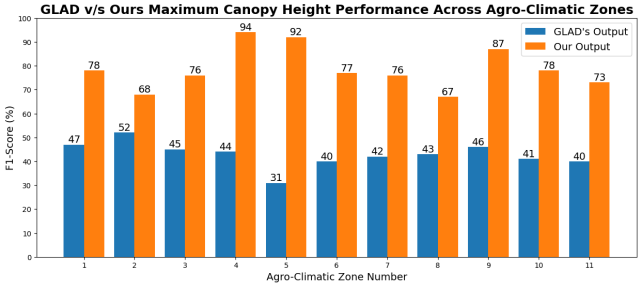


Figure 5: Maximum Canopy Height Prediction Comparison Between GLAD v/s Developed Models Across Different ACZ on July 2020 - December 2020 Data

analysis. For example, if the change between AY 2017 and AY 2021 needs to be assessed, then the modal output of AY 2016, 2017, and 2018 is taken as the starting year's health output and compared against the modal value of AY 2020, 2021 and 2022 as the final year's health output. Ground truth data for deforestation patches is gathered from the Indian Forest Clearance website and manually curated using the time-based imagery available on Google Earth Pro to identify patches that clearly show deforestation over the years [15]. No ground truth is however available for afforestation, improvement, or degradation changes in tree cover. Therefore, we show a comparison with existing baseline methods only for deforestation detection on the forest clearance ground truth patches. We also provide details on inferring overall tree health changes and also provide confidence scores associated with this change inference.

5.1 Afforestation/Deforestation Classification

The Dynamic World LULC tree cover mask was used to identify tree pixels across years. To analyze changes between a pair of years, if there was no tree cover in the first year and

[15] https://forestsclearance.nic.in/Online_Status.aspx

a tree cover in the second year, then that area is termed as afforested land. Similarly, if there was tree cover in the first year and no tree cover was detected in the second year, then that area is termed as deforested. The Forest Clearance website lists all the geo-tagged forest patches that are submitted and granted permission to be cleared, along with metadata about the purpose and details of the clearance. We observed that many forest patches that were granted clearance were still intact when visualizing the area on Google Earth Pro, and therefore we manually sifted through many patches to identify those for which we could clearly observe transition years within which the area had gone from afforested to deforested. A total of 1261 pixels of 25m resolution were obtained from across 8 patches from different ACZs, and used to evaluate the deforestation detection accuracy of our method. We were able to detect deforestation with a 97.86% accuracy. The following sub-sections compare the performance of our method against GLAD outputs and the BFast change detection methods.

5.1.1 Comparison with GLAD Outputs. GLAD uses Landsat and Sentinel satellites to provide tree cover loss outputs at a 30m resolution. The data outputs are available on GEE [22]. Therefore, GLAD's results were evaluated on the same ground-truth patches which formed 873 pixels at a 30m resolution. GLAD monitors tree sites that were classified as tree cover (plot with at least one tree with ≥3m canopy height) in 2000, and stops monitoring the site whenever it has a tree cover loss (≥50% canopy density loss). Additionally, GLAD only monitored tree cover gain from 2000 to 2012, and stopped monitoring after 2012. First, we observed that GLAD was monitoring just 30 out of the 873 tree pixels. On these 30 pixels, GLAD's deforestation detection accuracy was only 40%. The reason for such a low performance can be that the GLAD models are direct change detection models trained at a global scale, or they do not handle cases of missing data which are common when using Sentinel-1 SAR data. In comparison, our method did much better and were able to track all the pixels. Further, our method also tracks afforestation and improvements in the area.

5.1.2 Comparison with BFast Models. The BFast method is an advanced time series analysis technique designed to detect and characterize abrupt changes in vegetation indexes. It decomposes time series data into trend, seasonal, and remainder components, making it particularly effective to monitor environmental changes such as deforestation. We used the BFASTmonitor algorithm available on GEE to identify deforestation [20]. This BFast method uses Landsat satellite data's derived NDVI to detect breakpoints at a 30m resolution. The implementation of BFast that we used was able to generate outputs on only 102 out of 873 pixels though. On these pixels, BFast had a deforestation detection accuracy of 92.16% as compared to our method's accuracy of 97.86%. While the performance of BFAST is not very worse than our method, we feel that it in unable to provide an output on most pixels because it does not handle missing data effectively. Therefore, although BFast directly tries to infer change, it is sensitive to data quality issues. Our method which differences cross-sectional outputs of different years and fills missing data and corrects for fluctuations, appears to be more practical and less sensitive to poor data quality.

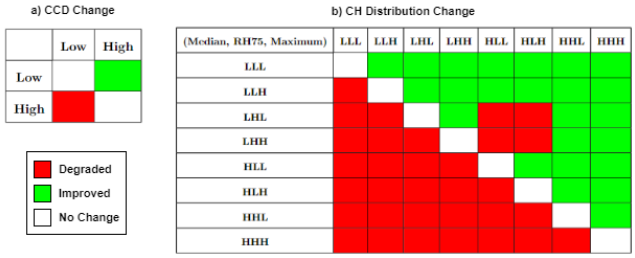


Figure 6: CCD and CH Distribution Change Inference Between 2 Years. Here, L: Low and H: High denote the output class for relative canopy height

5.2 Canopy Density Change Classification

We detect canopy density changes between a pair of years only if tree cover is present across the years. For a year, we compute the modal values of the CCD output in the previous year, current year, and next year, and then look at the difference between these modal values for the given pair of years. For example, to do a change analysis between AY 2017 and AY 2021, the modal CCD output (low/high) of AY 2016-2018 is taken as the value for AY 2017, and similarly the modal CCD output of AY 2020-2021 is taken as the value for AY 2021, and the change inference is done based on these values. Figure 6 a) shows this inference matrix of change between a given year-1 and year-2 of whether improvement or degradation or no change has taken place for canopy density.

5.3 Canopy Height Distribution Change Classification

Change inference for the CH distribution follows a similar strategy of using the modal values for a given year to infer change between a pair of years. The change inference is done based on the output classes obtained for the median, 75th percentile (RH75), and maximum tree height for the years. Figure 6 b) shows the inference matrix of change between a given year-1 and year-2 of whether improvement or degradation or no change has taken place for tree canopy height.

(CCD, CH)	Improved	Degraded	No Change
Improved			
Degraded			
No Change			

Figure 7: Overall Tree Health Change Between a Pair of Years, Based on CCD and Relative CH Outputs. (Green: Improved; Red: Degraded; Yellow: Partially Degraded; White: No Change)

5.4 Overall Tree Health Change Classification

Finally, we infer the overall tree health change based on whether CCD and CH has improved or degraded between a given pair of years. Figure 7 shows the inference matrix to obtain change classes of improvement (green), degradation (red), partially degradation (yellow), and no change (white). Rows show the CCD change classes and columns show the CH distribution change classes between a pair of years. If a tree site has the same change classes for CCD and CH, then the same change class is assigned to its overall health (E.g: CCD degradation and CH degradation indicates an overall degradation as well). If one of CCD or CH shows no change, then the health indicator of the other is assigned as the overall health change (E.g: An area with no change in CCD but an improvement in CH is marked as an overall improvement in health). If both of show no change, then the overall tree health also indicates no change. Finally, if one of the indicators shows improvement and the other shows degradation, then the output is marked as partial degradation, to favour detection of degradation on priority.

5.5 Confidence Level of Tree Health Change Inference

As discussed in section 4.3, a high or low confidence score is associated with the health output for each tree cover pixel based on the stability of the CCD and CH model predictions. Since change analysis is done on modal values of the given pair, to obtain the mode we also consider the confidence score of the years on which the modal value is computed. It can be inferred that the fluctuation correction rules explained earlier lead to a setup where (V - [!V] - ?) patterns over consecutive 3 years will either have all high or all low values. Consequently, there is no ambiguity in finding the modal value but we mark it as having low confidence. The only other pattern possible is a (V - V - V) combination when the confidence score of the output is high in all the years,

		Year 2	
		High	**Low**
Year 1	**High**	Low	Medium
	Low	Medium	Low

Table 4: Confidence Levels of the CCD and CH Changes Between the Modal Values of Year-1 (from year-1 minus one to year-1 plus one) and Year-2 (from year-2 minus one to year-2 plus one)

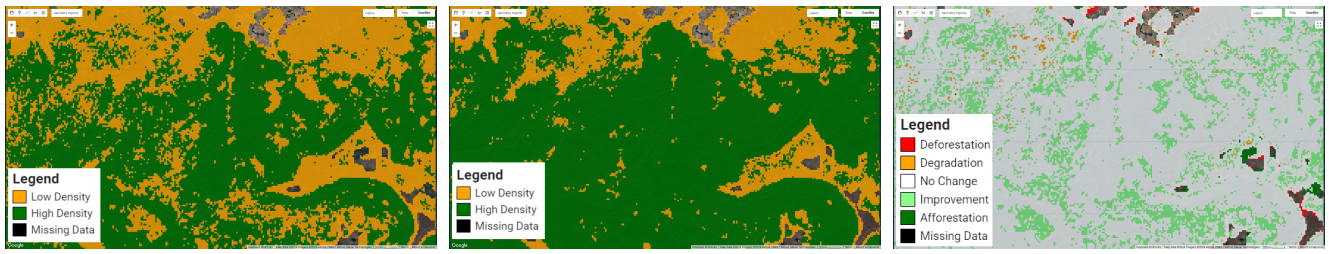
and therefore the modal value is also marked with a high confidence. These confidence levels of the modal values are used to assign a conference level to the inferred change between a pair of years. Table 4 shows the inference matrix to compute the confidence scores of the change inference, as high, medium, and low confidence scores. The row represents the confidence score of the modal year-1 output (from year-1 minus one to year-1 plus one) and the column represents the confidence score of the modal year-2 (from year-2 minus one to year-2 plus one). If the confidence score is high for both years, then the change output also has high confidence. If both years have low confidence scores, then the change output also has low confidence. Additionally, if one year has a high confidence output and another year has a low confidence output, then the change output is marked with medium confidence.

6 Trees Cover Health Analysis in India

This section illustrates various applications with being able to monitor tree health across different years and ACZs in India. The CCD and CH maps can be generated for any parts from AY 2016 using this approach because Sentinel-1&2 datasets are available from 2016 onwards. Furthermore, the changes in CCD, CH, and overall tree health can be detected using the inference methods discussed in section 5, and change maps can be generated across years for any region. We use this produce forest health change statistics across different ACZs in India.

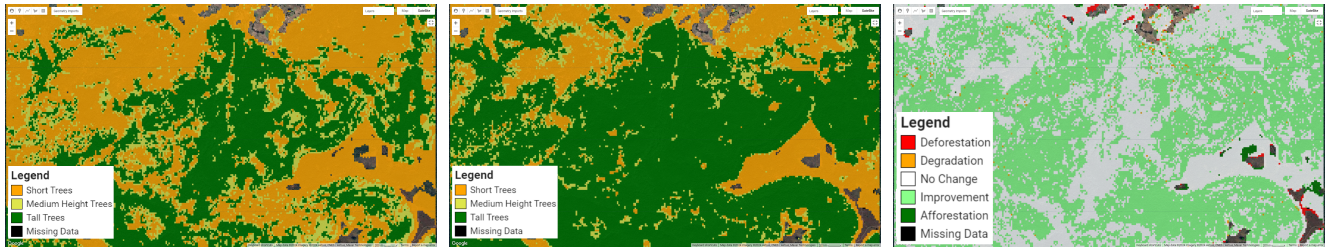
6.1 Tree Health Change Maps from AY 2017 to AY 2021

As a demonstration, this section shows the outputs of tree health in a forest patch in the Dongariya Village, situated in the Paraswada block of the Balaghat district in the state of Madhya Pradesh. A Google satellite view of the forest is shown in Figure 10a, which seems to primarily have a dense tree cover. The Balaghat district is known to be covered with 80% forest. Sal, Teak, and Bamboo are the major trees grown in this area.



(a) CCD Output for AY 2017 (b) CCD Output for AY 2021 (c) CCD Change from AY 2017 to 2021

Figure 8: CCD Output Maps for AY 2017 and AY 2021, as well as Change Maps of a Forest Patch Between these Years for Dongariya Village, Balaghat District, Madhya Pradesh



(a) CH Output for AY 2017 (b) CH Output for AY 2021 (c) CH Change from AY 2017 to 2021

Figure 9: CH Output Maps for AY 2017 and AY 2021, as well as Change Maps Between these Years of a Forest Patch in Dongariya Village, Balaghat District

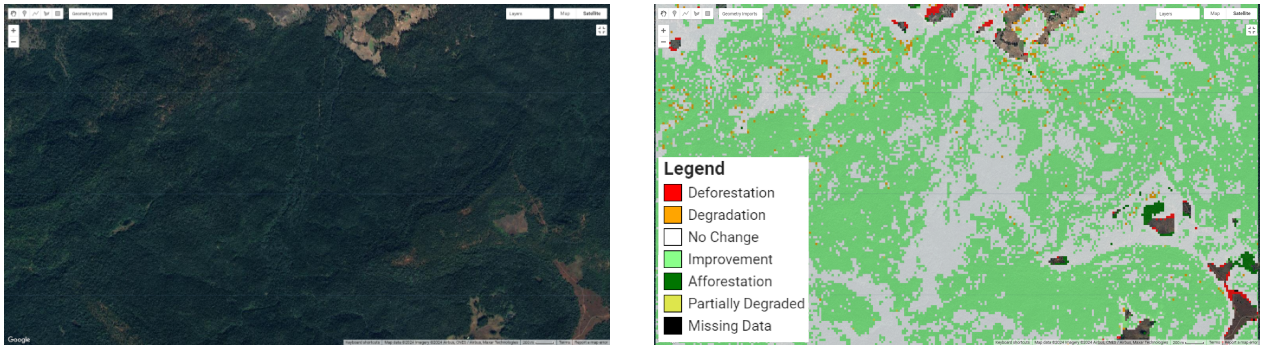
Figure 8 shows the CCD outputs in AY 2017 and AY 2021, and the CCD change maps between these years. It can be seen that the canopy density has improved significantly in this area, with slight degradation in some parts of the forest. There are a few small clusters of deforestation and afforestation patches which can be observed in the change maps. Figure 9 show the CH distribution maps for AY 2017 and AY 2021 years. It is inferred that the height of most of the trees has grown in this area from AY 2017 to AY 2021. Therefore, the overall tree health in this area has improved in most of the forest, as shown in Figure 10b. There are very few sites that show partial degradation in this region, where only one of the CCD or CH has improved and the other has degraded. There are also some parts where the overall health has degraded or there are no changes over the years.

Similarly, a forest area in the Boipariguda Village, Koraput District, Odisha was observed on Google Earth Pro in AY 2021, where a mix of dense tree cover and open forest area (low canopy cover) were observed, as shown in Figure 11a. Figure 11b represents the CCD model's output for AY 2021, which seems to be in line with the Google Pro image's observations. We can see from Figure 11c and Figure 11d that the model predicts a high canopy density in dense forest areas. The CCD output for low canopy density in the open forest area is also consistent with the map's observations, as seen in Figure 11e and Figure 11f. Therefore, the improvement and degradation changes based on the CCD model's output are also likely to be accurate.

A similar exercise was conducted to check our method's results on deforestation and afforestation patches. Figure 12 shows a forest patch obtained from the Forest Clearance website, which shows how the tree cover in AY 2018 and has been completely deforested in AY 2022. The change map shows the correct inference of deforestation between these years. Similar observations were made in other regions by comparing with Google Earth Pro images, wherever available, and the results from our methods were found to be consistent with the observations. Going forward, we are collaborating with several civil society organizations in India who have undertaken forest restoration activities, and are evaluating our results on sites where they are working.

6.2 Macro-Level Tree Health Changes in India from AY 2017 to AY 2021

We computed changes in tree health for all the 11 ACZs in India from AY 2017 to AY 2021. Table 5 shows aggregate statistics of the area of land afforested, deforested, improved, degraded, and partially degraded for all the ACZs in multiples of '000 hectares (kha). The partially degraded areas were further analyzed if they were the areas where CH degraded (and CCD improved) or CCD degraded (and CH improved). It was observed that ACZ-10, Southern Plateau and Hills



(a) Google Earth Engine Map **(b) Overall Tree Health Change**

Figure 10: Overall Tree Health Change Maps Between AY 2017 and AY 2021 of a Forest Patch in Dongariya Village, Balaghat District, Madhya Pradesh

Region (SPAHR) had the highest afforestation of 3,672 kha during this period. The ACZ-7, Eastern Plateau and Hills Region (EPAHR) recorded the highest deforestation of 2,281 kha, along with the highest degradation of 2,050 kha and an improvement of 3,487 kha. SPAHR reported the largest net change of 1,943 kha, which is computed as the difference between the amount of afforested and deforested land areas. ECPAHR had the next highest net change in tree cover of 1,003 kha. Additionally, ACZ-5, Upper Gangetic Plain Region (UGPR) accounts for the highest net loss of 688 kha. The ACZ-8, Central Plateau and Hills Region (CPAHR) shows highest partially degraded land while both CH and CCD show reverse trends. Partially degraded areas should ideally be less as compared to the areas that show complete improvement or degradation trends, and our reported statistics are in line with this hypothesis. It can also be seen that the scale of improved and degraded tree area across all ACZ is comparable to the amount of afforestation and deforestation. This highlights that our method enables tracking the changes in the trees at a small scale, which is crucial in analyzing the impact of carbon stock and climate change dynamics in the environment. Figure 13 demonstrates the tree health outputs for the CPAHR zone in AY 2021, and the overall tree health change map from AY 2017 to AY 2021, where we can observe a lot of tree growth has happened as quantified in the table. The tree health output maps for the rest of the ACZ are included in the subsection A.1.

Similarly, we also obtained district-wise statistics to identify the districts where highest growth or deterioration happened. Lakhimpur Kheri (170 kha), Jalgaon (154 kha), and Yavatmal (144 kha) districts saw the highest deforestation during the period. Adilabad (210 kha), Mayurbhanj (189 kha), and Y.S.R. (148 kha) were districts where higest tree degradation was noticed. Highest afforestation took place in Prakasam (242 kha), Belgaum (194 kha), and Chittoor (192 kha) districts. The higest improvement in trees was spotted in Khammam (229 kha), Betul (213 kha), and Chhindwara (208 kha). Additionally, the total change statistics in the districts were computed, which showed the difference between the total growth (afforested + improved) and the total deterioration (deforested + degraded + partially degraded) in a region. The Betul district in Madhya Pradesh saw the highest positive change of 177 kha, while the Mayurbhanj district in Odisha saw the lowest negative change of 141 kha. Reports indicate that a lot of restoration interventions took place in Madhya Pradesh during the 2017-18 period on degraded forest and urban tree plantation sites which led to an improvement in the tree health by 2021 [36]; this seems to be in line with our findings which show that highest improvements took place in MP's districts.

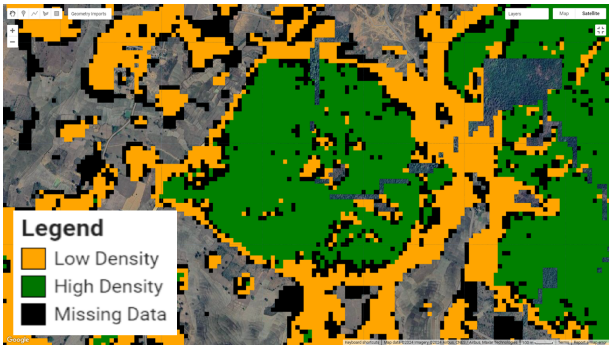
As another example, the Forest Survey of India Report 2021 indicates a large decline in mangrove trees in the Sundarban forests and the trees outside the forest region in North 24 Parganas and South 24 Parganas districts in West Bengal [37, 43, 56]. Our own analysis of this area also provides an assessment of total negative change of 168 kha.

7 Conclusion and Future Scope

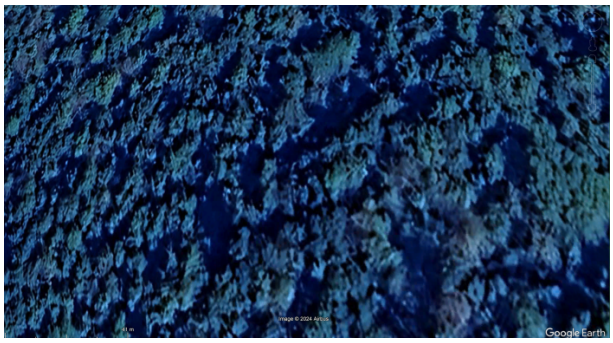
In this work, we developed spatiotemporally robust, open-source, and scalable methods for constantly monitoring the tree sites across India at small spatial scales, by estimating the CCD and CH distribution in a particular year, as well as changes across years. We compared our methods with existing baseline approaches and found that our models outperform all of them in India. We also demonstrated the output maps for different areas and compared them against the Google Earth Pro images, which seem in line with visual observations. The in-depth change analysis between AY 2017 and AY 2021 shows that high tree cover improvements took



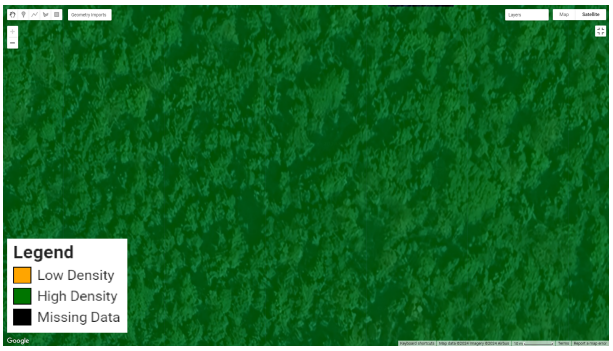
(a) Google Earth Pro Map of a Forest Patch



(b) CCD Output Map on Forest Patch



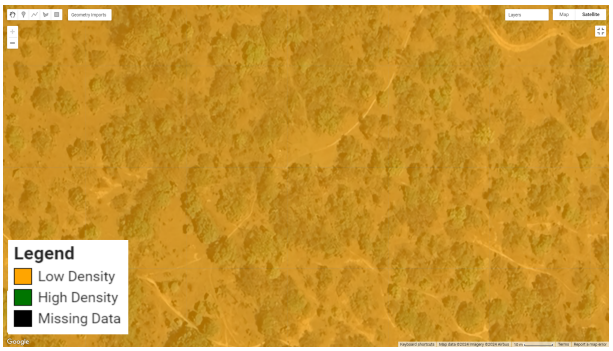
(c) Google Earth Map of Dense Forest



(d) CCD Model's Prediction as High Canopy Density



(e) Google Earth Map of Open Forest



(f) CCD Model's Prediction as Low Canopy Density

Figure 11: CCD Model's Results for AY 2021 in a Forest Patch of Boipariguda Village, Koraput District, Odisha

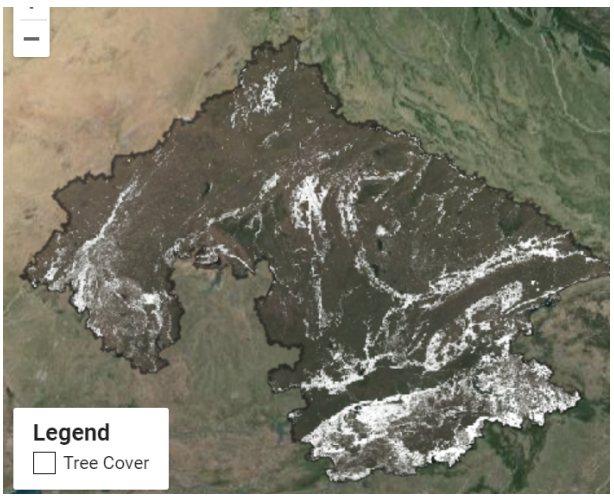
place in the Betul district of Madhya Pradesh (MP), corroborated by reports of multiple tree restoration interventions undertaken in the area during this time. Similar, trends were also observed in other districts of MP where restoration activities have taken place. A steep decline in the tree cover was also observed in the North 24 Parganas and South 24 Parganas districts, spanning the Sundarban forest regions in West Bengal, and corroborates with reports by the Forest Survey of India. Our outputs seem that they can be helpful for government and local forest communities to make scientifically backed decisions to identify sites for restoration and to track changes over time.

We aim to publish all our output maps and analysis in the Android application, Commons Connect, that will be openly accessible to people to monitor their areas of interest. This tool can also be leveraged by village forest protection committees to take appropriate actions in degraded areas and adopt best practices in improved areas for sustainability. It would also give access to higher state-level officials to view the aggregate maps and assess which parts are doing better or worse to plan appropriate actions. These outputs can also be used to estimate the health of forest areas where Community Forest Rights (CFRs) have been granted, and help the forest communities and the Forest Department to

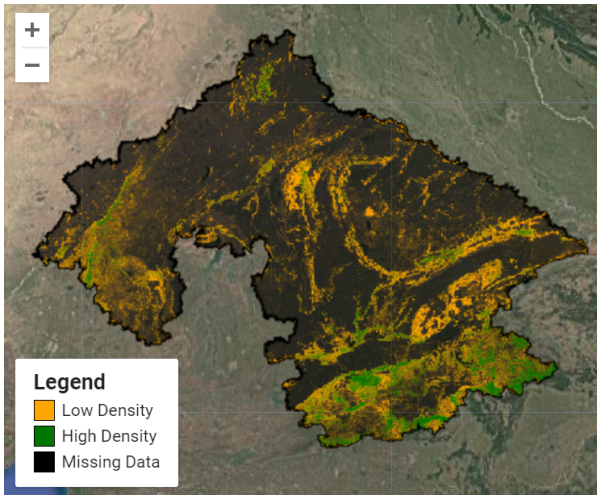


(a) Google Earth Image of AY 2018 (b) Google Earth Image of AY 2022 (c) Deforestation Change Prediction

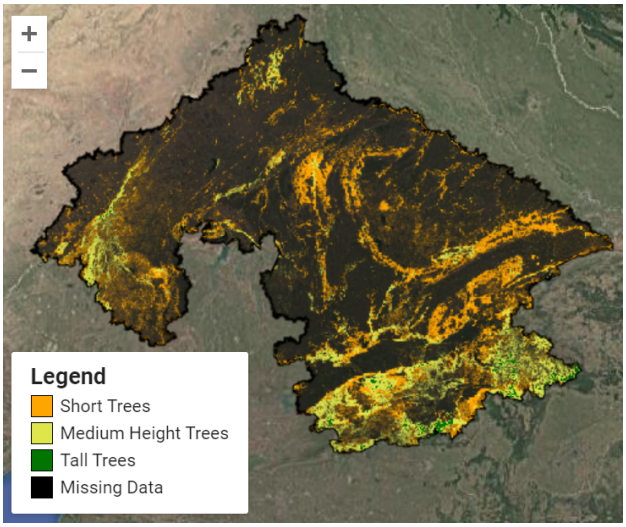
Figure 12: Google Earth Pro Images and Change Map on a forest patch that was cleared between AY 2018 to AY 2022



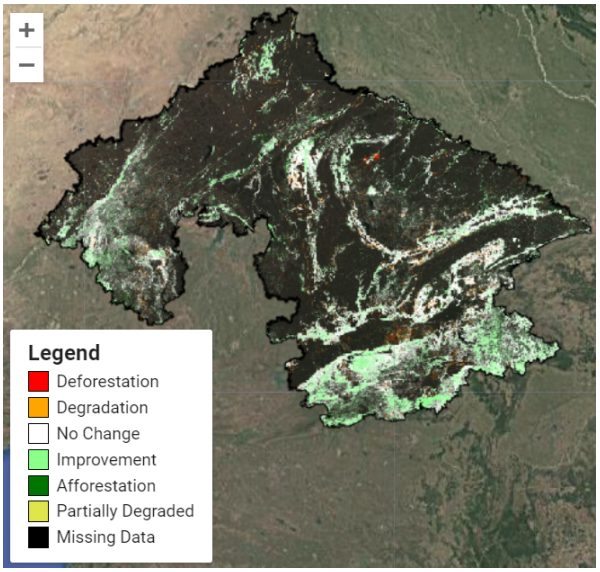
(a) Tree Cover in AY 2021



(b) CCD Outputs for AY 2021



(c) CH Outputs for AY 2021



(d) Overall Tree Health Change from AY 2017 to 2021

Figure 13: Tree Health Output Maps for Central Plateau and Hills Region

ACZ Number	Afforested	Deforested	Improved	Degraded	Partially Degraded	
					CCD Improved, CH Degraded	CCD Degraded, CH Improved
1	887	367	367	417	20	21
2	1,083	859	1,466	1,179	74	118
3	530	366	482	652	57	34
4	1,006	1,552	309	204	6	5
5	565	1,253	1,058	733	25	7
6	87	156	97	116	6	6
7	2,286	2,281	3,487	2,050	50	56
8	1,319	1,050	1,961	643	65	51
9	2,115	1,700	1,448	1,326	67	110
10	3,672	1,729	1,450	1,561	142	54
11	1,982	979	862	780	69	24

Table 5: Tree Health Change Statistics (in '000 hectares) of All Agro-Climatic Zone from AY 2017 to AY 2021

plan appropriate actions. We are also working on segregating results in terms of changes in Large Tree Patches (LTP) of more than one hectare and Short Tree Patches (STP) of small-area plantations, to get a better understanding of whether improvement or degradation has happened in forests or in trees outside forests. These results are likely to inform debates about how forest departments distinguish between forests and plantations, and whether they offset degradation statistics of ecologically rich forests with improvements in monoculture plantations on private land [24, 31, 32].

Acknowledgments

We would like to thank Tower Research, GIZ, and Tarides for supporting the research, and the Foundation for Ecological Security (FES) and the Jharkhand Jungle Bachao Andolan (JJBA) for facilitating field visits to ground the research.

References

[1] Mabel Ortega Adarme, Raul Queiroz Feitosa, Patrick Nigri Happ, Claudio Aparecido De Almeida, and Alessandra Rodrigues Gomes. 2020. Evaluation of Deep Learning Techniques for Deforestation Detection in the Brazilian Amazon and Cerrado Biomes From Remote Sensing Imagery. *Remote Sensing* 12 (2020), 910. Issue 6. https://doi.org/10.3390/rs12060910

[2] K. Baker, I. S. Miguel, and T. Jones. 2020. FARM-TRACE Approved Approach for Automated Forests & Carbon Assessments. https://www.planvivo.org/news/farm-trace-public-consultation by Plan Vivo; accessed on 10 January 2024.

[3] Asim Banskota, Nilam Kayastha, Michael J. Falkowski, Michael A. Wulder, Robert E. Froese, and Joanne C. White. 2014. Forest Monitoring Using Landsat Time Series Data: A Review. *Canadian Journal of Remote Sensing* 40 (2014), 362–384. Issue 5. https://doi.org/10.1080/07038992.2014.987376

[4] John Brandt and Fred Stolle. 2021. A global method to identify trees outside of closed-canopy forests with medium-resolution satellite imagery. *International Journal of Remote Sensing* 42 (2021), 1713–1737. Issue 5. https://doi.org/10.1080/01431161.2020.1841324

[5] Christopher F. Brown, Steven P. Brumby, Brookie Guzder-Williams, Tanya Birch, Samantha Brooks Hyde, Joseph Mazzariello, Wanda Czerwinski, Valerie J. Pasquarella, Robert Haertel, Simon Ilyushchenko, Kurt Schwehr, Mikaela Weisse, Fred Stolle, Craig Hanson, Oliver Guinan, Rebecca Moore, and Alexander M. Tait. 2022. Dynamic World, Near real-time global 10 m land use land cover mapping. *Scientific Data* 9, 251 (2022). https://doi.org/10.1038/s41597-022-01307-4

[6] Tudor Buhalau. 2016. Detecting clear-cut deforestation using Landsat data : a time series analysis of remote sensing data in Covasna County, Romania between 2005 and 2015. *Student thesis series Ines* (2016). https://api.semanticscholar.org/CorpusID:133122993

[7] Allan Buras, Anja Rammig, and Christian S. Zang. 2021. The European Forest Condition Monitor: Using Remotely Sensed Forest Greenness to Identify Hot Spots of Forest Decline. *Frontiers in Plant Science* 12 (2021). https://doi.org/10.3389/fpls.2021.689220

[8] Press Information Bureau. 2018. Cooperation of Society in Implementation of Redd+ Strategy is Crucial. https://pib.gov.in/newsite/PrintRelease.aspx?relid=183155 published by Ministry of Environment, Forest and Climate Change, Government of India; accessed on 7 December 2023.

[9] Ben DeVries, Arun Kumar Pratihast, Jan Verbesselt, Lammert Kooistra, Sytze de Bruin, and Martin Herold. 2013. Near real-time tropical forest disturbance monitoring using Landsat time series and local expert monitoring data. In *MultiTemp 2013: 7th International Workshop on the Analysis of Multi-temporal Remote Sensing Images*. IEEE, 1–4. https://doi.org/10.1109/Multi-Temp.2013.6866022

[10] Hoang Huu Dinh, Shyam Basnet, and Alec Zuo. 2024. Impact of tree planting on household well-being: evidence from the central highlands of Vietnam. *Environmental Systems Research* 13, 1 (2024), 11. https://doi.org/10.1186/s40068-024-00331-0

[11] Ralph Dubayah, James Bryan Blair, Scott Goetz, Lola Fatoyinbo, Matthew Hansen, Sean Healey, Michelle Hofton, George Hurtt, James Kellner, Scott Luthcke, John Armston, Hao Tang, Laura Duncanson, Steven Hancock, Patrick Jantz, Suzanne Marselis, Paul L. Patterson, Wenlu Qi, and Carlos Silva. 2020. The Global Ecosystem Dynamics Investigation: High-resolution laser ranging of the Earth's forests and topography. *Science of Remote Sensing* 1 (2020), 100002. https://doi.org/10.1016/j.srs.2020.100002

[12] Saeedeh Eskandari, Mohammad Reza Jaafari, Patricia Oliva, Omid Ghorbanzadeh, and Thomas Blaschke. 2020. Mapping Land Cover and Tree Canopy Cover in Zagros Forests of Iran: Application of Sentinel-2, Google Earth, and Field Data. *Remote Sensing* 12 (2020), 1912. Issue 12. https://doi.org/10.3390/rs12121912

[13] Saeedeh Eskandari and Sajjad Ali Mahmoudi Sarab. 2022. Mapping land cover and forest density in Zagros forests of Khuzestan province in Iran: A study based on Sentinel-2, Google Earth and field data. *Ecological Informatics* 70 (2022), 101727. https://doi.org/10.1016/j.ecoinf.2022.101727

[14] Saulo Folharini, Sarah Moura Batista dos Santos, António Bento-Gonçalves, and António Vieira. 2022. Estimation of Tree Height in Burned Areas with GEDI Laser Data in Northern Portugal and Galicia (Spain). *Environmental Sciences Proceedings* (2022), 50. https://doi.org/10.3390/IECF2022-13050

[15] Tenaw Geremew, Alemu Gonsamo, Worku Zewdie, and Petri Pellikka. 2023. Extrapolation of canopy height and cover metrics of GEDI LiDAR in tropical montane forest ecosystem. *African Geographical Review* (2023), 1–17. https://doi.org/10.1080/19376812.2023.2164865

[16] Ebrahim Ghaderpour and Tijana Vujadinovic. 2020. Change Detection within Remotely Sensed Satellite Image Time Series via Spectral Analysis. *Remote Sensing* 12 (2020), 4001. Issue 23. https://doi.org/10.3390/rs12234001

[17] Sujit M. Ghosh, Mukunda D. Behera, Subham Kumar, Pulakesh Das, Ambadipudi J. Prakash, Prasad K. Bhaskaran, Parth S. Roy, Saroj K. Barik, Chockalingam Jeganathan, Prashant K. Srivastava, and Soumit K. Behera. 2022. Predicting the Forest Canopy Height from LiDAR and Multi-Sensor Data Using Machine Learning over India. *Remote Sensing* 14 (2022), 5968. Issue 23. https://doi.org/10.3390/rs14235968

[18] Sujit Madhab Ghosh, Mukunda Dev Behera, and Somnath Paramanik. 2020. Canopy Height Estimation Using Sentinel Series Images through Machine Learning Models in a Mangrove Forest. *Remote Sensing* 12 (2020), 1519. Issue 9. https://doi.org/10.3390/rs12091519

[19] Holly K Gibbs, Sandra Brown2, John O Niles3, and Jonathan A Foley. 2007. Monitoring and estimating tropical forest carbon stocks: making REDD a reality. *Environmental Research Letters* 2, 4 (10 2007), 045023. https://doi.org/10.1088/1748-9326/2/4/045023

[20] Eliakim Hamunyela, Sabina Rosca, Andrei Mirt, Eric Engle, Martin Herold, Fabian Gieseke, and Jan Verbesselt. 2020. Implementation of BFASTmonitor Algorithm on Google Earth Engine to Support Large-Area and Sub-Annual Change Monitoring Using Earth Observation Data. *Remote Sensing* 12, 18 (2020), 2953. https://doi.org/10.3390/rs12182953

[21] Matthew C Hansen, Alexander Krylov, Alexandra Tyukavina, Peter V Potapov, Svetlana Turubanova, Bryan Zutta, Suspense Ifo, Belinda Margono, Fred Stolle, and Rebecca Moore. 2016. Humid tropical forest disturbance alerts using Landsat data. *Environmental Research Letters* 11 (2016), 034008. Issue 3. https://doi.org/10.1088/1748-9326/11/3/034008

[22] M. C. Hansen, P. V. Potapov, R. Moore, M. Hancher, S. A. Turubanova, A. Tyukavina, D. Thau, S. V. Stehman, S. J. Goetz, T. R. Loveland, A. Kommareddy, A. Egorov, L. Chini, C. O. Justice, and J. R. G. Townshend. 2013. High-Resolution Global Maps of 21st-Century Forest Cover Change. *Science* 342, 6160 (2013), 850–853. https://doi.org/10.1126/science.1244693

[23] Xiaolan Huang, Weicheng Wu, Tingting Shen, Lifeng Xie, Yaozu Qin, Shanling Peng, Xiaoting Zhou, Xiao Fu, Jie Li, Zhenjiang Zhang, Ming Zhang, Yixuan Liu, Jingheng Jiang, Penghui Ou, Wenchao Huangfu, and Yang Zhang. 2021. Estimating Forest Canopy Cover by Multiscale Remote Sensing in Northeast Jiangxi, China. *Land 2021* 10 (2021), 433. Issue 4. https://doi.org/10.3390/land10040433

[24] Shuchita Jha. 2022. Plantations, invasive species... what all India counts as 'forest'. https://www.downtoearth.org.in/forests/plantations-invasive-species-what-all-india-counts-as-forest--81282 published by Down To Earth; accessed on 10 July 2024.

[25] Patrick Kacic, Andreas Hirner, and Emmanuel Da Ponte. 2021. Fusing Sentinel-1 and -2 to Model GEDI-Derived Vegetation Structure Characteristics in GEE for the Paraguayan Chaco. *Remote Sensing* 13 (2021), 5105. Issue 24. https://doi.org/10.3390/rs13245105

[26] Lauri Korhonen, Hadi, Petteri Packalen, and Miina Rautiainen. 2017. Comparison of Sentinel-2 and Landsat 8 in the estimation of boreal forest canopy cover and leaf area index. *Remote Sensing of Environment* 195 (2017), 259–274. https://doi.org/10.1016/j.rse.2017.03.021

[27] Nico Lang, Nikolai Kalischek, John Armston, Konrad Schindler, Ralph Dubayah, and Jan Dirk Wegner. 2022. Global canopy height regression and uncertainty estimation from GEDI LIDAR waveforms with deep ensembles. *Remote Sensing of Environment* 268 (2022), 112760. https://doi.org/10.1016/j.rse.2021.112760

[28] Zhanmang Liao, Albert I.J.M. Van Dijk, Binbin He, Pablo Rozas Larraondo, and Peter F. Scarth. 2020. Woody vegetation cover, height and biomass at 25-m resolution across Australia derived from multiple site, airborne and satellite observations. *International Journal of Applied Earth Observation and Geoinformation* 93 (2020), 102209. https://doi.org/10.1016/j.jag.2020.102209

[29] Aobo Liu, Xiao Cheng, and Zhuoqi Chen. 2021. Performance evaluation of GEDI and ICESat-2 laser altimeter data for terrain and canopy height retrievals. *Remote Sensing of Environment* 264 (2021), 112571. https://doi.org/10.1016/j.rse.2021.112571

[30] Jérôme Louis, Bringfried Pflug, Magdalena Main-Knorn, Vincent Debaecker, Uwe Mueller-Wilm, Rosario Quirino Iannone, Enrico Giuseppe Cadau, Valentina Boccia, and Ferran Gascon. 2019. Sentinel-2 Global Surface Reflectance Level-2a Product Generated with Sen2Cor. In *IGARSS 2019 - 2019 IEEE International Geoscience*

and Remote Sensing Symposium. 8522–8525. https://doi.org/10.1109/IGARSS.2019.8898540

[31] MD Madhusudan. 2022. How India counts its forest cover. https://mdmadhusudan.medium.com/how-india-counts-its-forest-cover-e8a41314c835 published on Medium; accessed on 10 July 2024.

[32] MD Madhusudan. 2022. Missing the forest for the trees. https://mdmadhusudan.medium.com/missing-the-forest-for-the-trees-37a94c13ab8c published on Medium; accessed on 10 July 2024.

[33] Lonesome Malambo, Sorin Popescu, and Meng Liu. 2023. Landsat-Scale Regional Forest Canopy Height Mapping Using ICESat-2 Along-Track Heights: Case Study of Eastern Texas. *Remote Sensing* 15 (2023). Issue 1. https://doi.org/10.3390/rs15010001

[34] Shivani A Mehta, Aila Dutt, Ajay Tannirkulam, Akshay Pratap Singh, Aman Verma, Anamitra Singha, Ananda Sreenidhi, Ananjan Nandi, Ankit, Ankit Kumar, Atharv Dabli, Athira P, Balakumaran Ramachandran, Chahat Bansal, Chintan Sanjaybhai Sheth, Craig Dsouza, Deepak Kumar, Dharmisha Sharma, Harshita, Jaskaran Singh, Kapil Dadheech, Ksheetiz Agrahari, Om Krishna, Pooja Prasad, Priyadarshini Radhakrishnan, Ramita Sardana, Rittwick Bhabak, Ruptirumal Sai Bodavula, Saketh Vishnubhatla, Samitha Haldar, Sanjali Agrawal, Shiv Prakash Maurya, Shruti Kumari, Siddharth S, Sukriti Kumari, Vishnu S, and Aaditeshwar Seth. 2024. Initial Observations from Field Testing of a Digital Participatory Tool to Improve Water Security in Rural India. (2024). To appear in ICTD, 2024.

[35] Edward Mitchard. 2016. *The Hectares Indicator: A Review of Earth Observation Methods for Detecting and Measuring Forest Change in the Tropics*. Vol. 1. Ecometrica. Edinburgh, UK. https://ecometrica.com/wp-content/uploads/2016/12/Review-of-EO-Methods-for-Detecting-and-Measuring-Forest-Change-in-the-Tropics-Final.pdf online; accessed on 5 February 2024.

[36] Wing-Green India Mission MP Forest Department. [n. d.]. Forest Landscape Based Planning & Restoration Initiatives Under Green India Mission - A Comprehensive Progress Report (Year 2017 to 2021). https://mpforest.gov.in/img/files/GIM_Comprehensive%20_Report.pdf online; accessed on 3 July 2024.

[37] Krishnendu Mukherjee. 2022. Kolkata loses 30% green cover in 10 years, Bengal less than 1% in two years. https://timesofindia.indiatimes.com/city/kolkata/kolkata-loses-30-green-cover-in-10-years-bengal-less-than-1-in-two-years/articleshow/93787328.cms published by Times of India; accessed on 5 July 2024.

[38] Vahid Nasiri, Ali Asghar Darvishsefat, Hossein Arefi, Verena C. Griess, Seyed Mohammad Moein Sadeghi, and Stelian Alexandru Borz. 2022. Modeling Forest Canopy Cover: A Synergistic Use of Sentinel-2, Aerial Photogrammetry Data, and Machine Learning. *Remote Sensing* 14 (2022), 1453. Issue 6. https://doi.org/10.3390/rs14061453

[39] Arun Nath, Brajesh Tiwari, Gudeta Sileshi, Uttam Sahoo, Biplab Brahma, Sourabh Deb, Ningthoujam Devi, Ashesh Das, Demsai Reang, Shiva Chaturvedi, Om Tripathi, Dhruba Das, and Asha Gupta. 2019. Allometric Models for Estimation of Forest Biomass in North East India. *Forests* 10 (2019), 103. Issue 2. https://doi.org/10.3390/f10020103

[40] United Nations. 2016. United Nations Sustainable Development Goals Strategic Plan 2030. https://unstats.un.org/sdgs online; accessed on 10 October 2023.

[41] Maeve Naughton-Rockwell. 2022. *Using Deep Learning with Satellite Imagery to Estimate Deforestation Rates*. Master's thesis. Undergraduate Honors Theses. William & Mary. https://scholarworks.wm.edu/honorstheses/1855

[42] Prateep K. Nayak. 2003. Community-Based Forest Management In India: The Significance Of Tenure. *Forests, Trees and Livelihoods* 13 (2003), 135–160. Issue 2. https://doi.org/10.1080/14728028.2003.9752451

[43] Forest Survey of India. 2021. *Forest Survey Report 2021*. Technical Report. Forest Department of India. https://fsi.nic.in/forest-report-2021-details

[44] Ministry of Tribal Affairs. 2006. Forest Rights Act. https://forestrights.nic.in/ForestRightAct.jsp# online; accessed on 1 December 2023.

[45] United Nations Framework Convention on Climate Change. [n. d.]. Estimation of carbon stocks and change in carbon stocks of trees and shrubs in A/R CDM project activities. https://cdm.unfccc.int/methodologies/ARmethodologies/tools/ar-am-tool-14-v4.2.pdf online; accessed on 3 December 2023.

[46] United Nations Framework Convention on Climate Change. 2015. Measurements for Estimation of Carbon Stocks in Afforestation and Reforestation Project Activities under the Clean Development Mechanism. https://unfccc.int/resource/docs/publications/cdm_afforestation_field-manual_web.pdf online; accessed on 3 December 2023.

[47] Ramesh Pandey. 2021. India Can Leverage its Forest Cover to Boost Climate Action, Support Global Mitigation Efforts. https://www.news18.com/news/opinion/india-can-leverage-its-forest-cover-to-boost-climate-action-support-global-mitigation-efforts-4414583.html published by News 18; accessed on 10 November 2023.

[48] Peter Potapov, Xinyuan Li, Andres Hernandez-Serna, Svetlana Turubanova, Alexandra Tyukavina, Matthew C. Hansen, Hao Tang, and Quyen Hanh Nguyen. 2021. Tropical Forest Canopy Structure and Change Assessment Using Landsat, GEDI, and Airborne Lidar Data. In *2021 IEEE International Geoscience and Remote Sensing Symposium IGARSS*. IEEE, 666–669. https://doi.org/10.1109/IGARSS47720.2021.9554814

[49] Peter Potapov, Xinyuan Li, Andres Hernandez-Serna, Alexandra Tyukavina, Matthew C. Hansen, Anil Kommareddy, Amy Pickens, Svetlana Turubanova, Hao Tang, Carlos Edibaldo Silva, John Armston, Ralph Dubayah, J. Bryan Blair, and Michelle Hofton. 2021. Mapping global forest canopy height through integration of GEDI and Landsat data. *Remote Sensing of Environment* 253 (2021), 112165. https://doi.org/10.1016/j.rse.2020.112165

[50] Maryam Pourshamsi, Mariano Garcia, Marco Lavalle, and Heiko Balzter. 2018. A Machine-Learning Approach to PolInSAR and LiDAR Data Fusion for Improved Tropical Forest Canopy Height Estimation Using NASA AfriSAR Campaign Data. *IEEE Journal of Selected Topics in Applied Earth Observations and Remote Sensing* 11 (2018). Issue 10. https://doi.org/10.1109/JSTARS.2018.2868119

[51] N. H. Ravindranath and Indu K. Murthy. 2018. *Estimation of carbon sequestration under MGNREGA: Achievement and Potential in India*. Technical Report. Department for International Development, New Delhi. https://assets.publishing.service.gov.uk/media/5cefa31b40f0b650d8050688/NREGA_Carbon_Sequestration_Report.pdf

[52] Khaldoun Rishmawi, Chengquan Huang, Karen Schleeweis, and Xiwu Zhan. 2022. Integration of VIIRS Observations with GEDI-Lidar Measurements to Monitor Forest Structure Dynamics from 2013 to 2020 across the Conterminous United States. *Remote Sensing* 14 (2022), 2320. Issue 10. https://doi.org/10.3390/rs14102320

[53] Khaldoun Rishmawi, Chengquan Huang, and Xiwu Zhan. 2021. Monitoring Key Forest Structure Attributes across the Conterminous United States by Integrating GEDI LiDAR Measurements and VIIRS Data. *Remote Sensing* 13 (2021), 442. Issue 3. https://doi.org/10.3390/rs13030442

[54] Fabian D. Schneider, António Ferraz, Steven Hancock, Laura I. Duncanson, Ralph O. Dubayah, Ryan P. Pavlick, and David S. Schimel. 2020. Towards mapping the diversity of canopy structure from space with GEDI. *Environmental Research Letters* 15 (2020). Issue 11. https://doi.org/10.1088/1748-9326/ab9e99

[55] A.K. Singh, C. Sahu, and S.K. Sahu. 2020. Carbon sequestration potential of a teak plantation forest in the Eastern Ghats of India. *Journal of Environmental Biology* 41 (2020), 770–775. Issue 4. https://doi.org/10.22438/jeb/41/4/MRN-1230

[56] Joydeep Thakur. 2022. Sunderbans losing its dense mangrove cover: Govt report. https://www.hindustantimes.com/india-news/sunderbans-losing-its-dense-mangrove-cover-govt-report-101642099620808.html published by Hindustan Times; accessed on 5 July 2024.

[57] Ramón Torres, Paul Snoeij, Malcolm Davidson, David Bibby, and Svein Lokas. 2012. The Sentinel-1 mission and its application capabilities. In *2012 IEEE International Geoscience and Remote Sensing Symposium*. 1703–1706. https://doi.org/10.1109/IGARSS.2012.6351196

[58] Kuimi T. Vashum. 2012. Methods to Estimate Above-Ground Biomass and Carbon Stock in Natural Forests - A Review. *Journal of Ecosystem & Ecography* 02 (2012). Issue 04. https://doi.org/10.4172/2157-7625.1000116

[59] Astrid Verhegghen, Klara Kuzelova, Vasileios Syrris, Hugh Eva, and Frédéric Achard. 2022. Mapping Canopy Cover in African Dry Forests from the Combined Use of Sentinel-1 and Sentinel-2 Data: Application to Tanzania for the Year 2018. *Remote Sensing* 14 (2022), 1522. Issue 6. https://doi.org/10.3390/rs14061522

[60] Cangjiao Wang, Andrew J. Elmore, Izaya Numata, Mark A. Cochrane, Lei Shaogang, Jiu Huang, Yibo Zhao, and Yuanyuan Li. 2022. Factors affecting relative height and ground elevation estimations of GEDI among forest types across the conterminous USA. *GIScience and Remote Sensing* 59 (2022). Issue 1. https://doi.org/10.1080/15481603.2022.2085354

[61] Geoff Wells, Janet A. Fisher, Ina Porras, Sam Staddon, and Casey Ryan. 2017. Rethinking Monitoring in Smallholder Carbon Payments for Ecosystem Service Schemes: Devolve Monitoring, Understand Accuracy and Identify Co-benefits. *Ecological Economics* 139 (2017), 115–127. https://doi.org/10.1016/j.ecolecon.2017.04.012

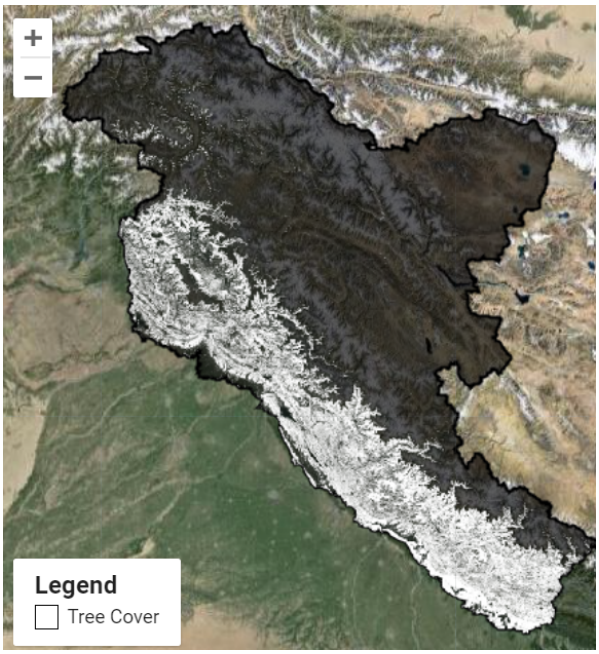
[62] Thales A. P. West, Jan Börner, Erin O. Sills, and Andreas Kontoleon. 2020. Overstated carbon emission reductions from voluntary REDD+ projects in the Brazilian Amazon. *Proceedings of the National Academy of Sciences* 117 (2020), 24188–24194. Issue 39. https://doi.org/10.1073/pnas.2004334117

[63] Tanjia Binte Zafar, Wenguang Ding, Shakir Ul Din, Ghulam Murtaza Khan, Chen Hao, and Li He. 2021. Forest cover and land use map of the Chunati Wildlife Sanctuary based on participatory mapping and satellite images: Insight into Chunati beat. *Land Use Policy* 103 (2021), 105193. https://doi.org/10.1016/j.landusepol.2020.105193

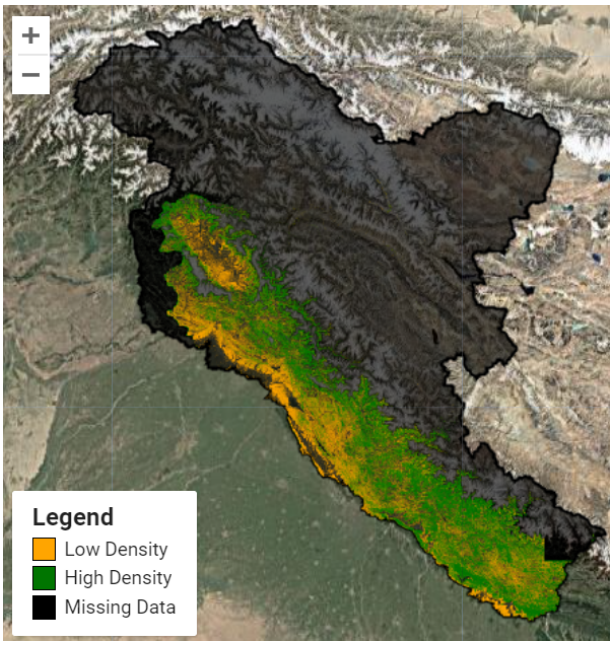
[64] Daniele Zanaga, Ruben Van De Kerchove, Wanda De Keersmaecker, Niels Souverijns, Carsten Brockmann, Ralf Quast, Jan Wevers, Alex Grosu, Audrey Paccini, Sylvain Vergnaud, Oliver Cartus, Maurizio Santoro, Steffen Fritz, Ivelina Georgieva, Myroslava Lesiv, Sarah Carter, Martin Herold, Linlin Li, Nandin-Erdene Tsendbazar, Fabrizio Ramoino, and Olivier Arino. 2021. ESA WorldCover 10 m 2020 v100. https://doi.org/10.5281/zenodo.5571936 dataset hosted by Zenodo.

A Appendix

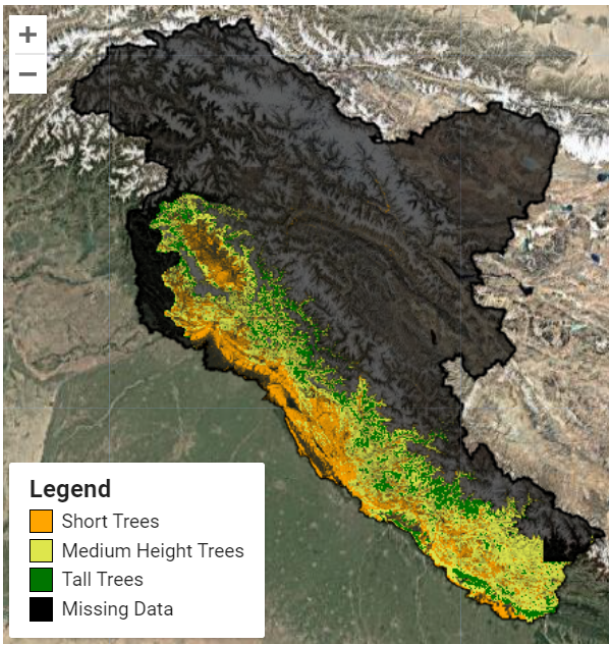
A.1 Tree Health Output Maps for Different ACZ in India



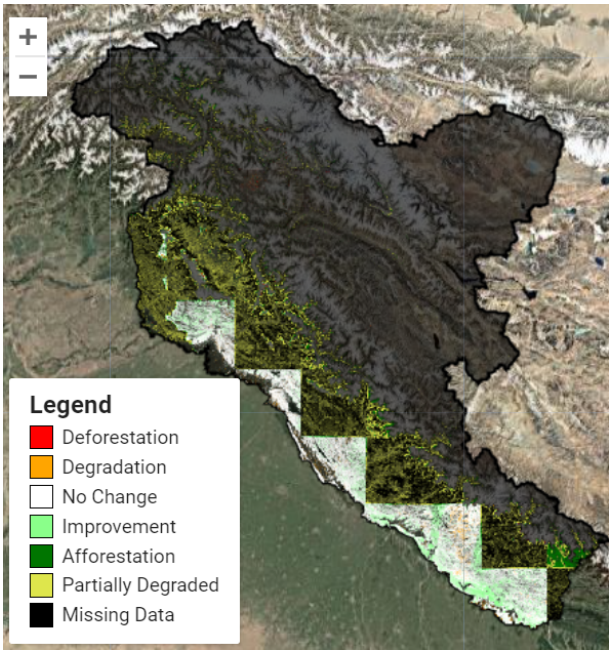
(a) Tree Cover in AY 2021



(b) CCD Outputs for AY 2021

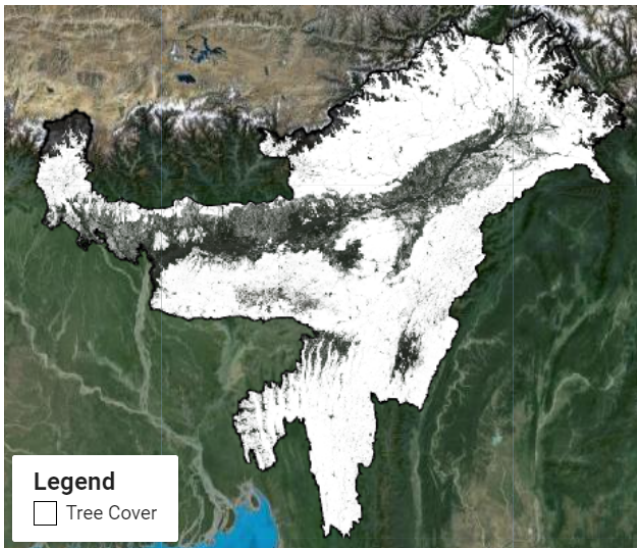


(c) CH Outputs for AY 2021

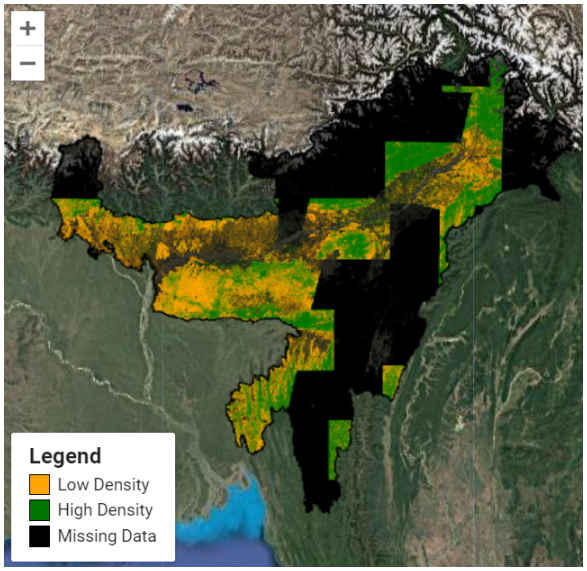


(d) Overall Tree Health Change from AY 2017 to 2021

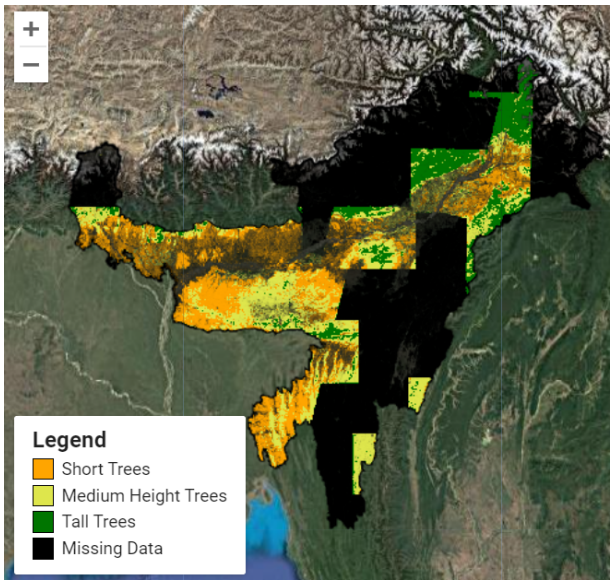
Figure 14: Tree Health Output Maps for Western Himalayan Region



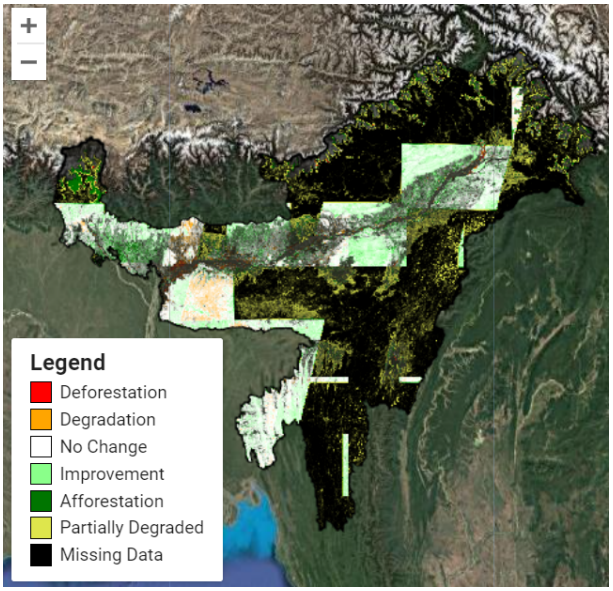
(a) Tree Cover in AY 2021



(b) CCD Outputs for AY 2021

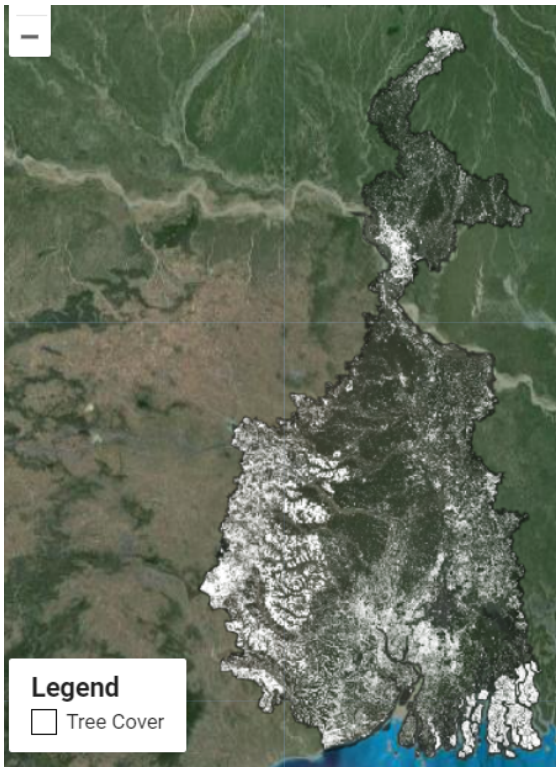


(c) CH Outputs for AY 2021

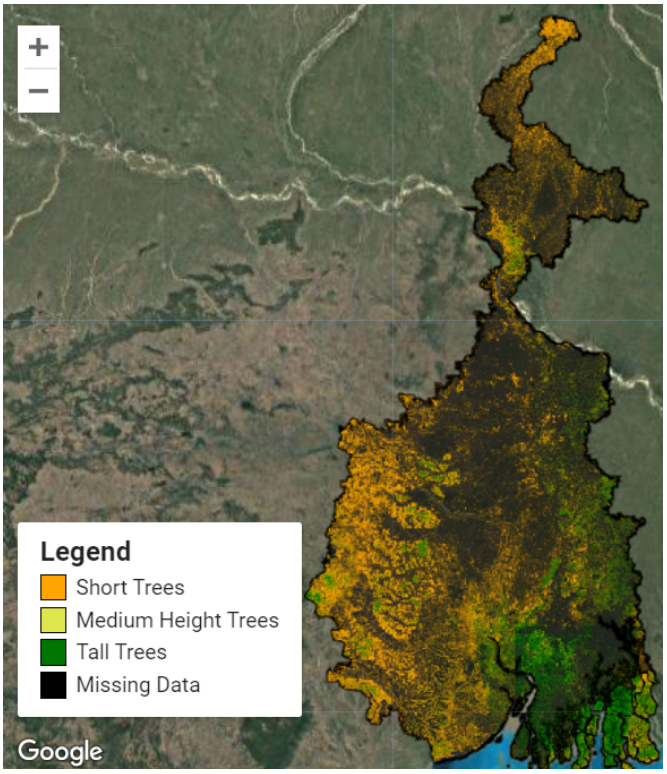


(d) Overall Tree Health Change from AY 2017 to 2021

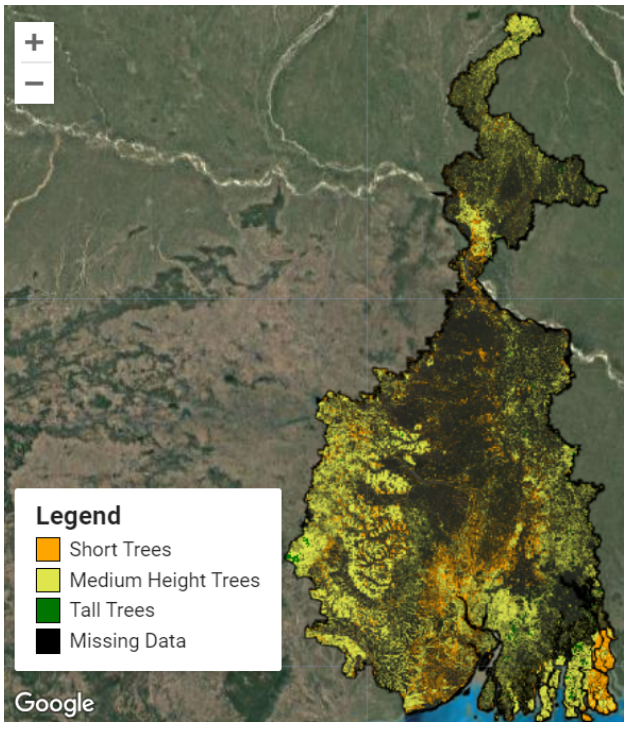
Figure 15: Tree Health Output Maps for Eastern Himalayan Region



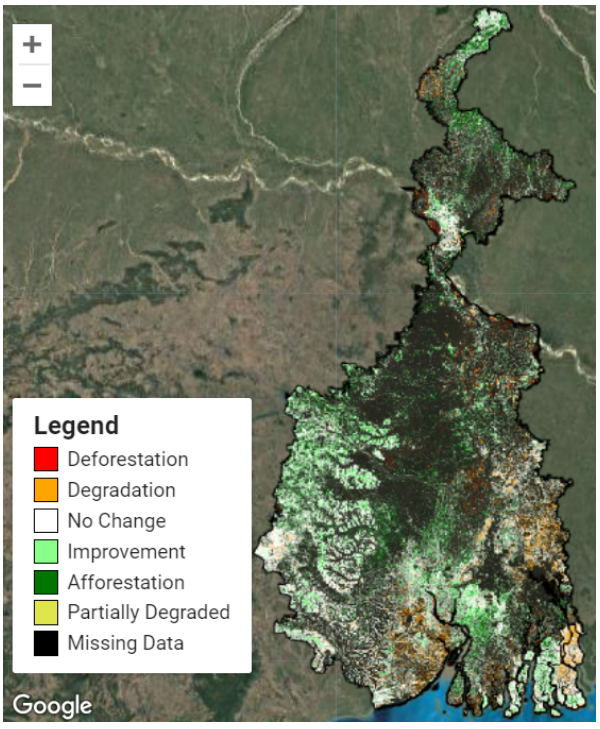
(a) Tree Cover in AY 2021



(b) CCD Outputs for AY 2021

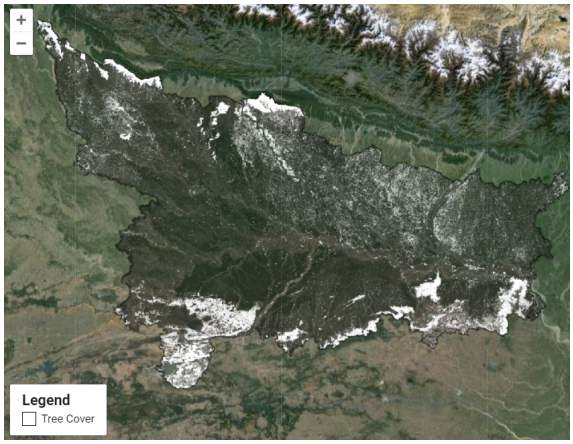


(c) CH Outputs for AY 2021

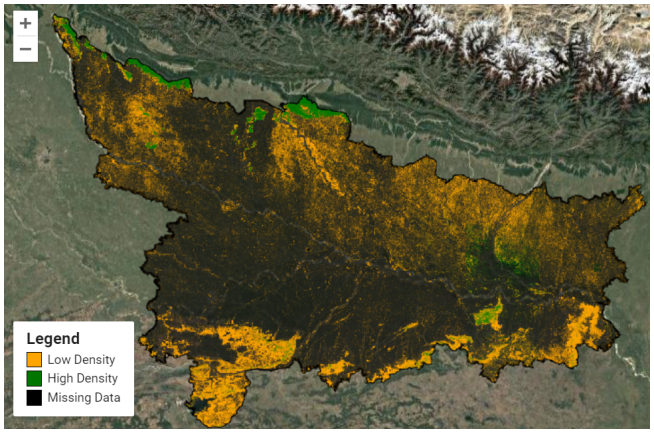


(d) Overall Tree Health Change from AY 2017 to 2021

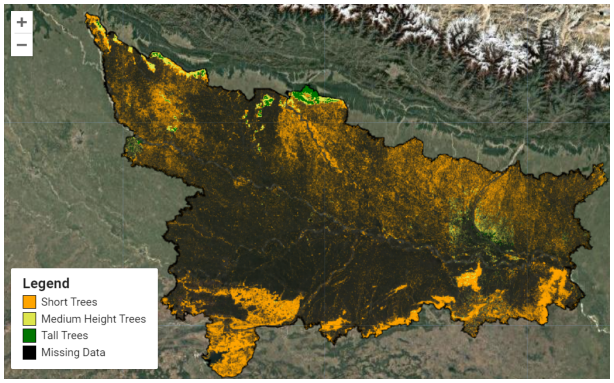
Figure 16: Tree Health Output Maps for Lower Gangetic Plain Region



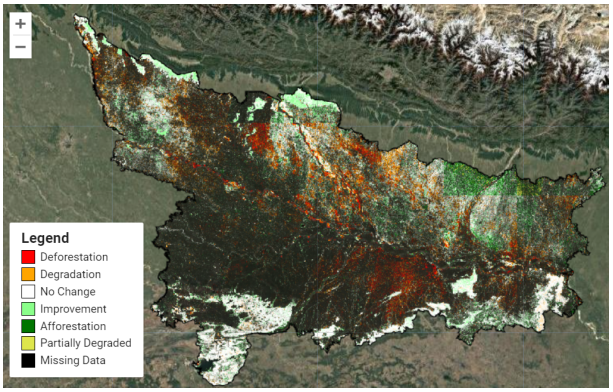
(a) Tree Cover in AY 2021



(b) CCD Outputs for AY 2021

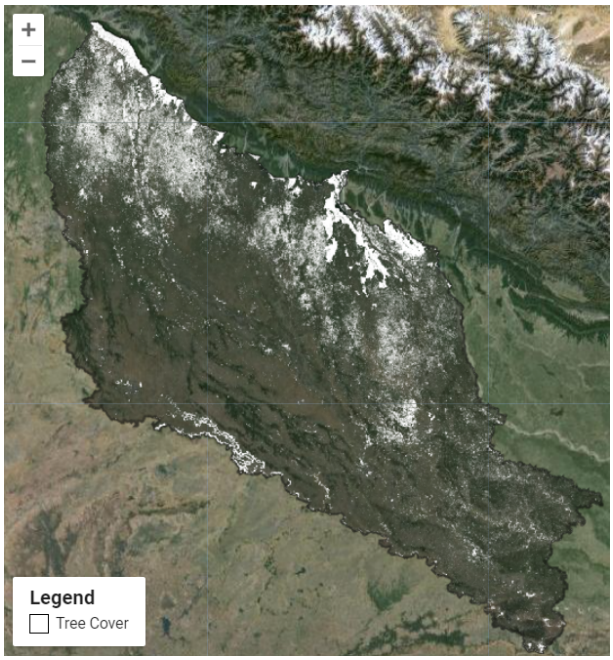


(c) CH Outputs for AY 2021

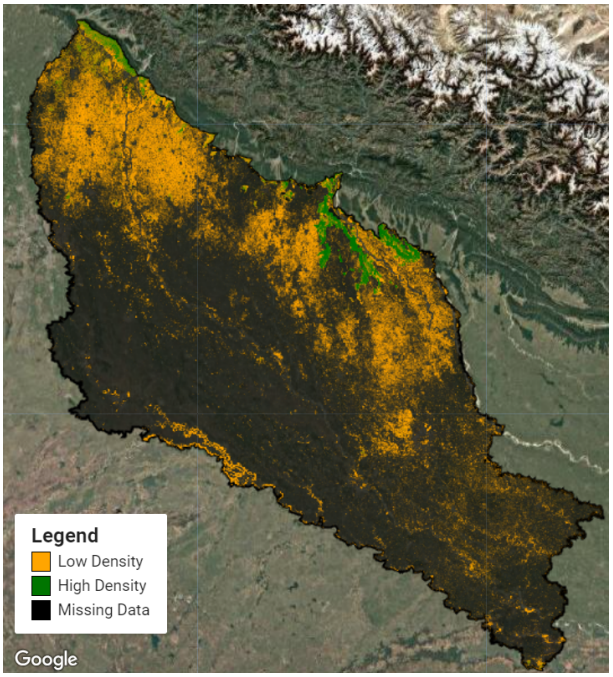


(d) Overall Tree Health Change from AY 2017 to 2021

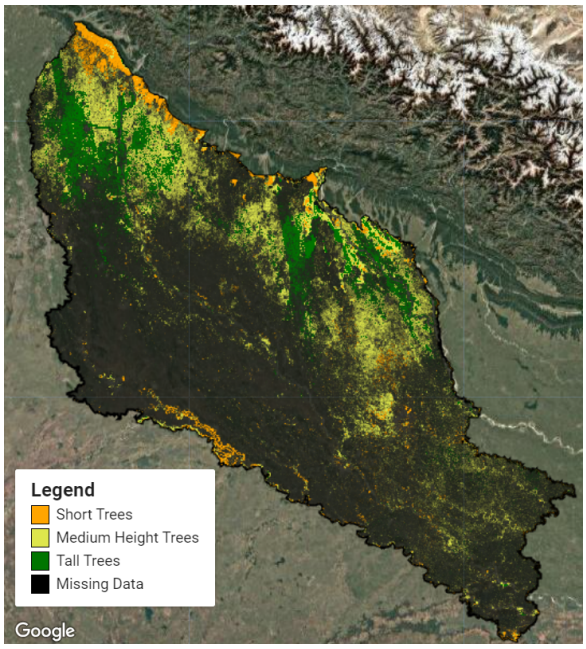
Figure 17: Tree Health Output Maps for Middle Gangetic Plain Region



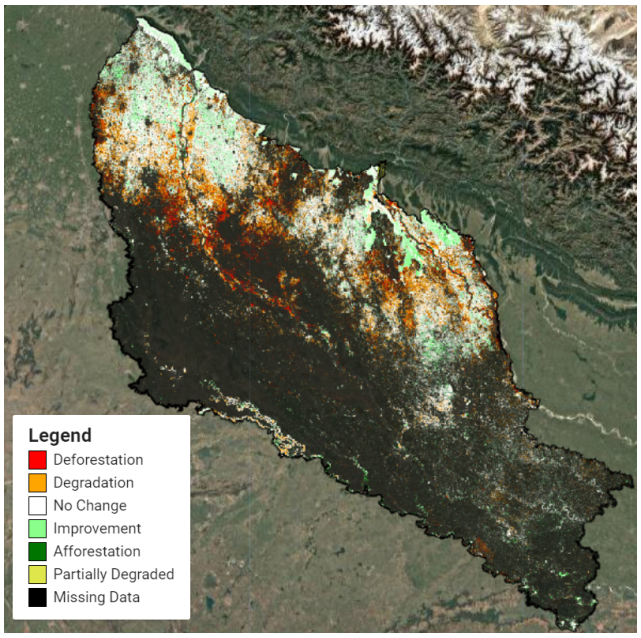
(a) Tree Cover in AY 2021



(b) CCD Outputs for AY 2021

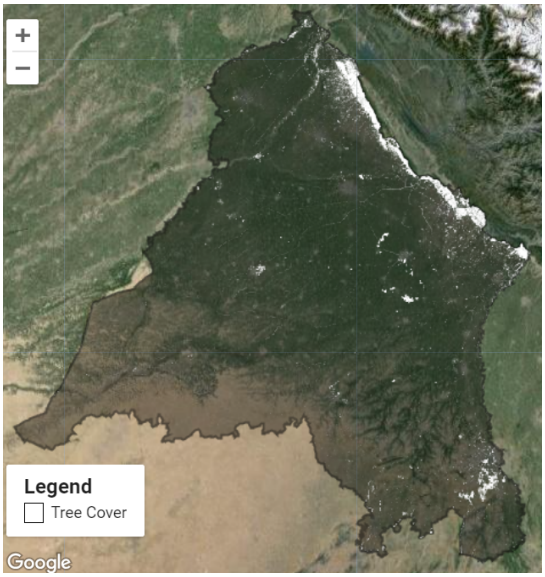


(c) CH Outputs for AY 2021

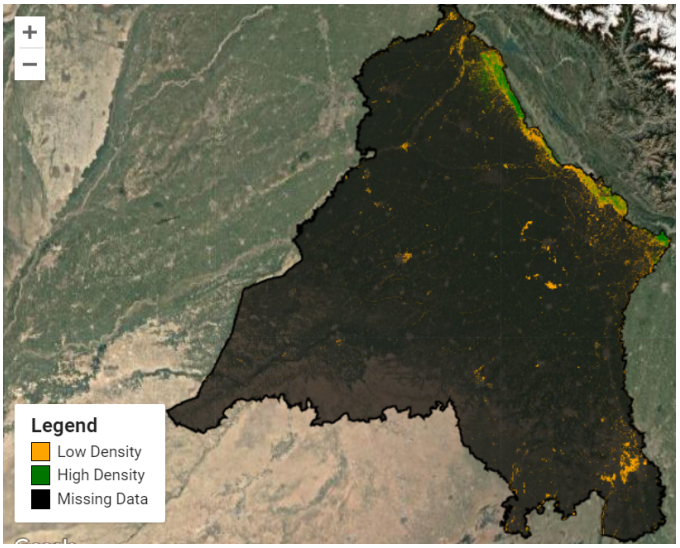


(d) Overall Tree Health Change from AY 2017 to 2021

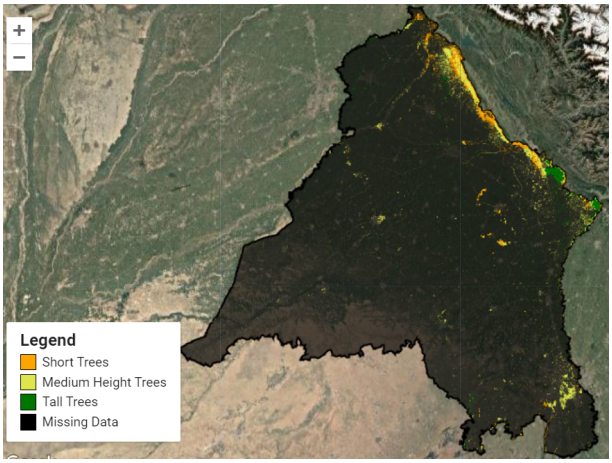
Figure 18: Tree Health Output Maps for Upper Gangetic Plain Region



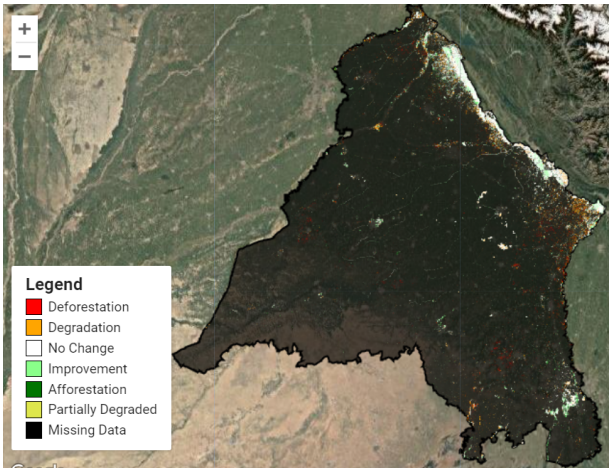
(a) Tree Cover in AY 2021



(b) CCD Outputs for AY 2021

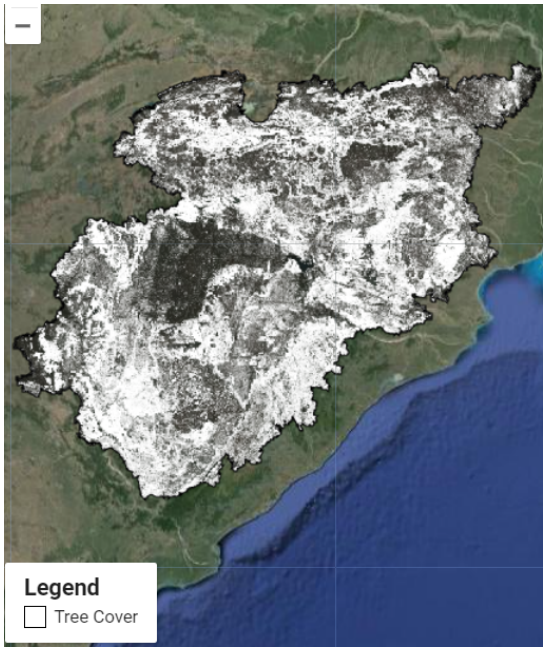


(c) CH Outputs for AY 2021

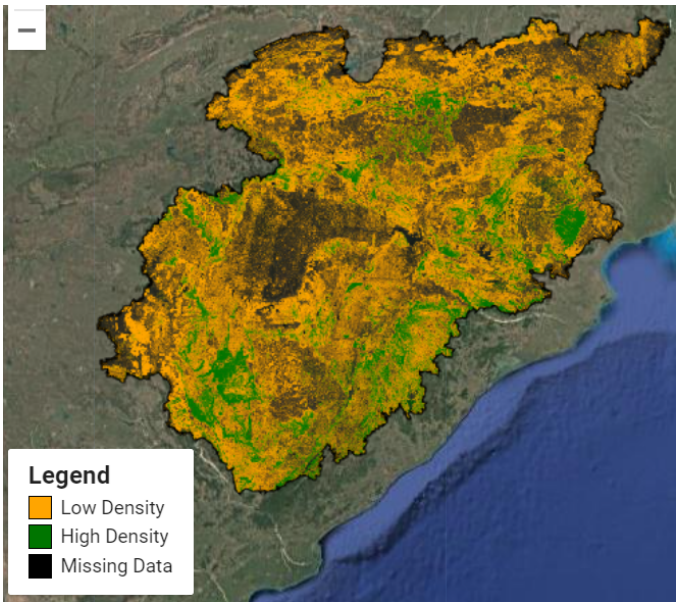


(d) Overall Tree Health Change from AY 2017 to 2021

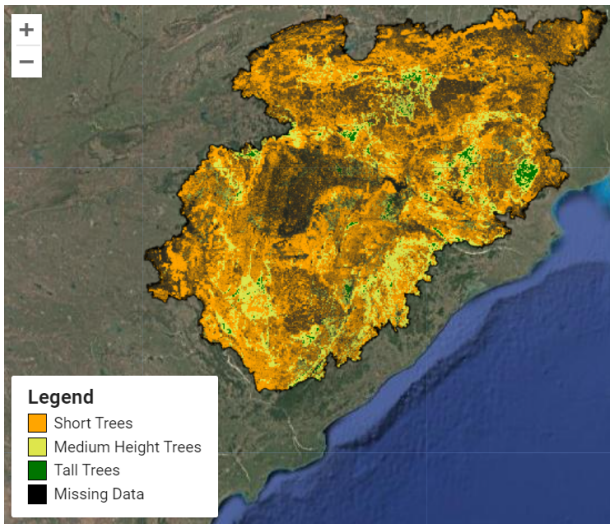
Figure 19: Tree Health Output Maps for Trans Gangetic Plain Region



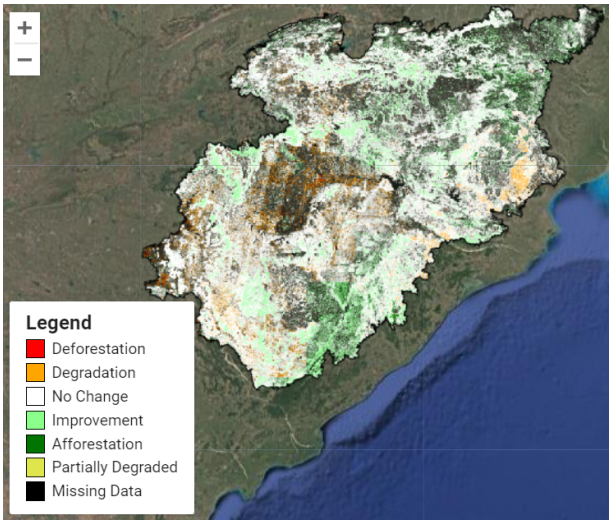
(a) Tree Cover in AY 2021



(b) CCD Outputs for AY 2021

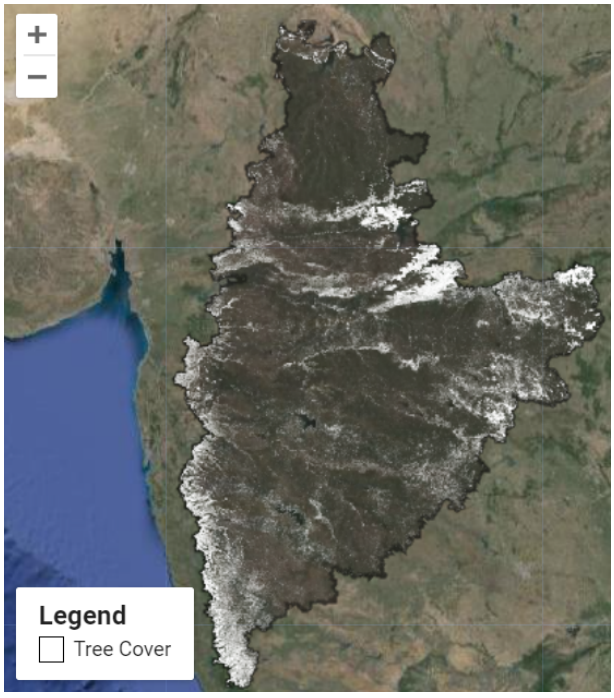


(c) CH Outputs for AY 2021

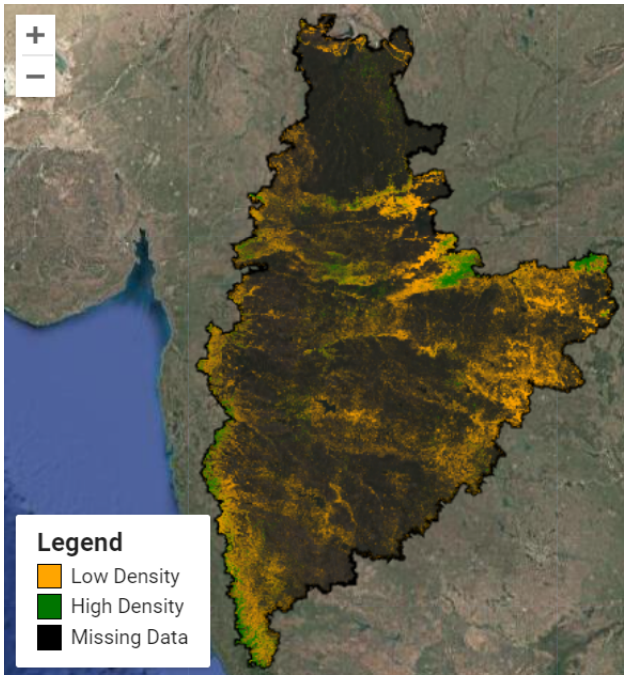


(d) Overall Tree Health Change from AY 2017 to 2021

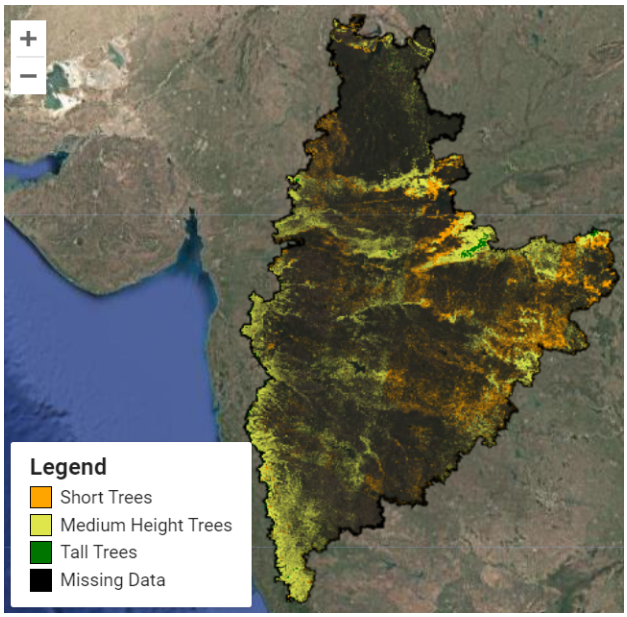
Figure 20: Tree Health Output Maps for Eastern Plateau and Hills Region



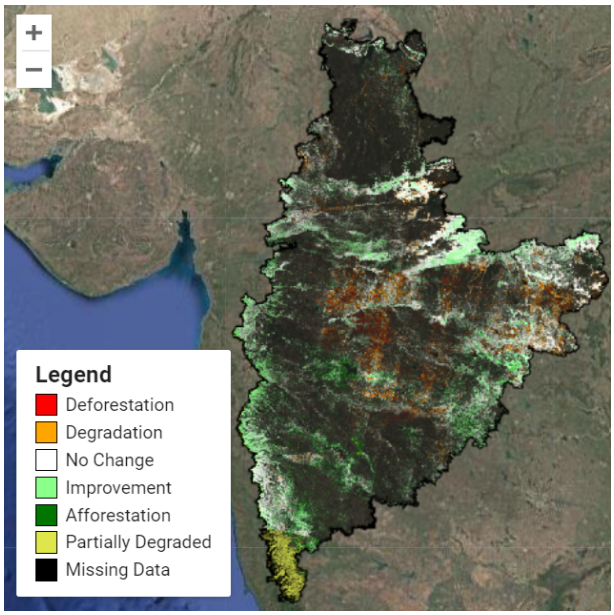
(a) Tree Cover in AY 2021



(b) CCD Outputs for AY 2021

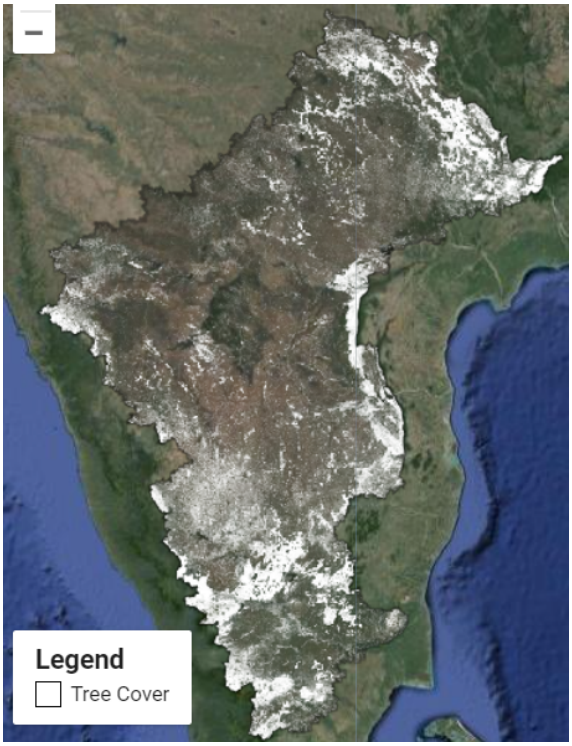


(c) CH Outputs for AY 2021

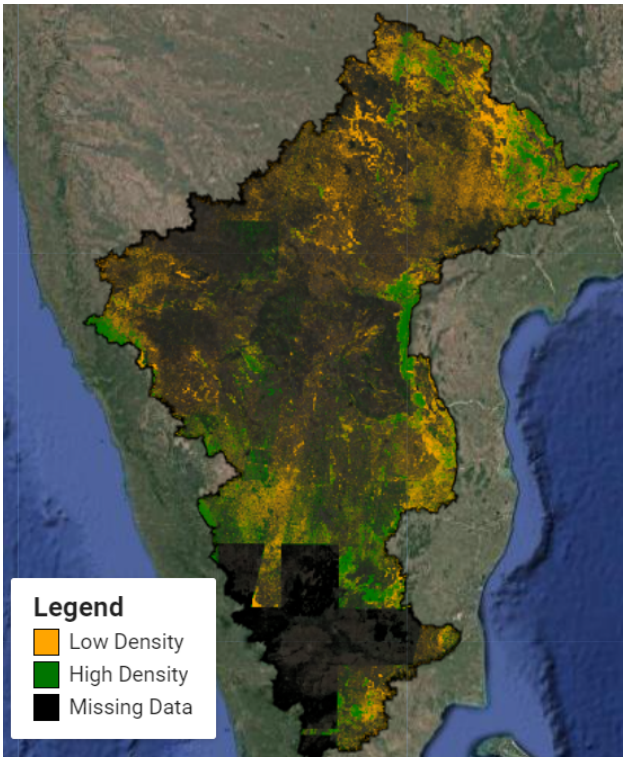


(d) Overall Tree Health Change from AY 2017 to 2021

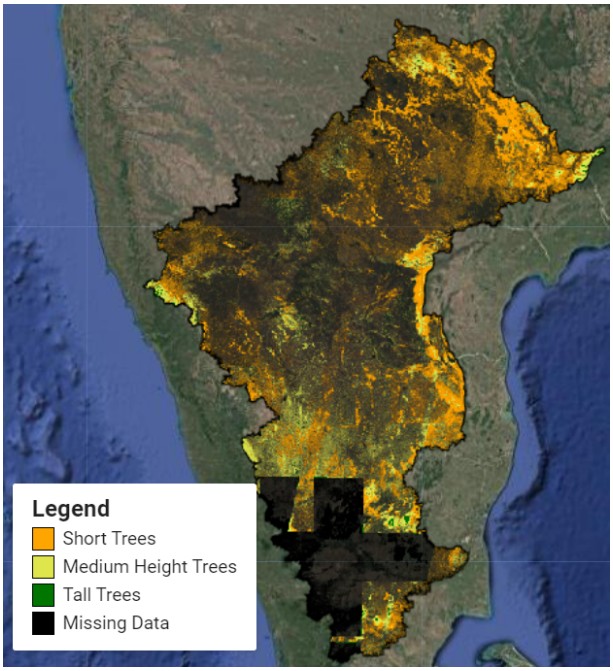
Figure 21: Tree Health Output Maps for Western Plateau and Hills Region



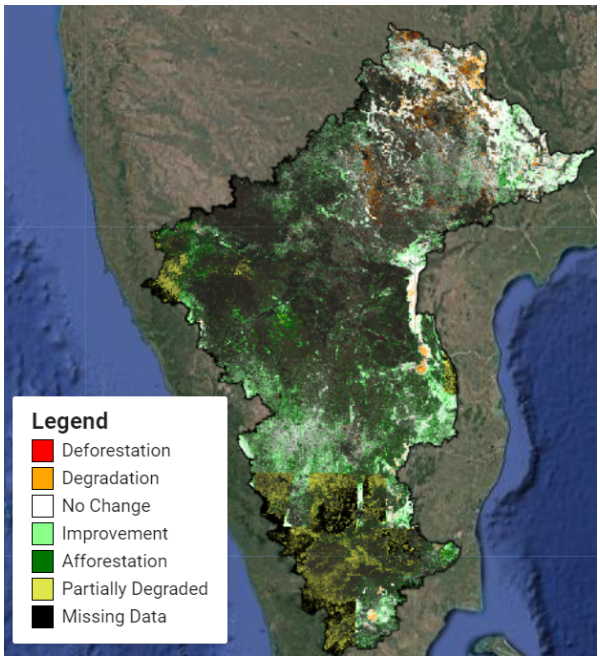
(a) Tree Cover in AY 2021



(b) CCD Outputs for AY 2021

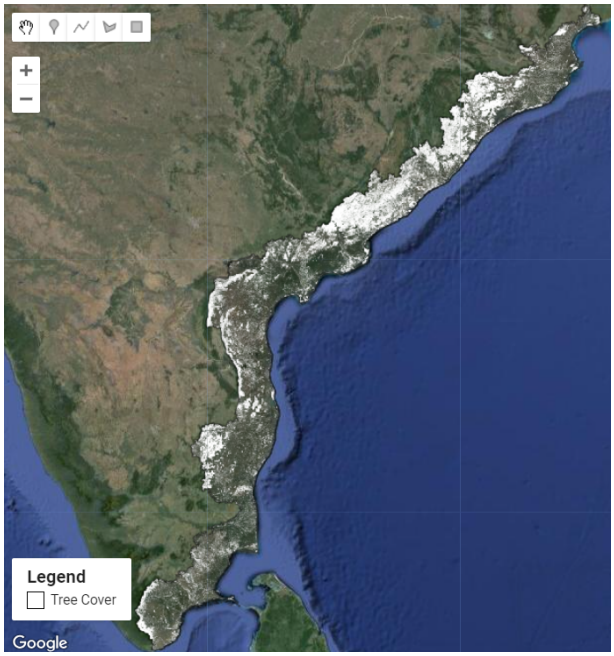


(c) CH Outputs for AY 2021

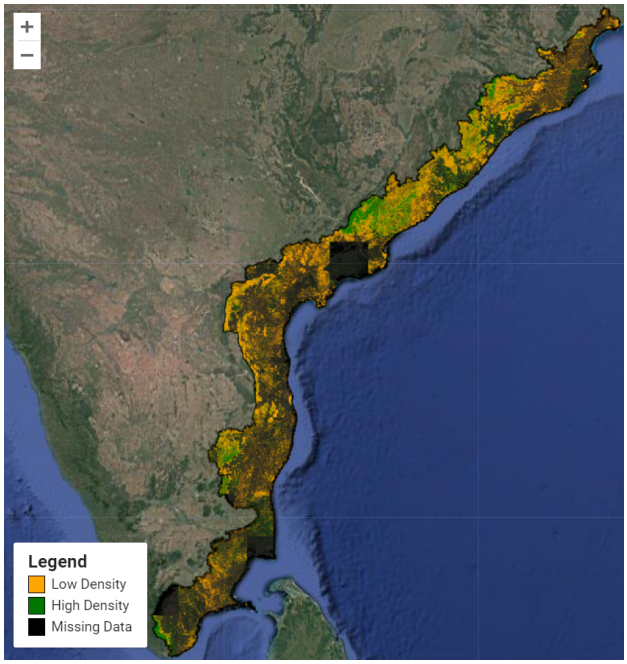


(d) Overall Tree Health Change from AY 2017 to 2021

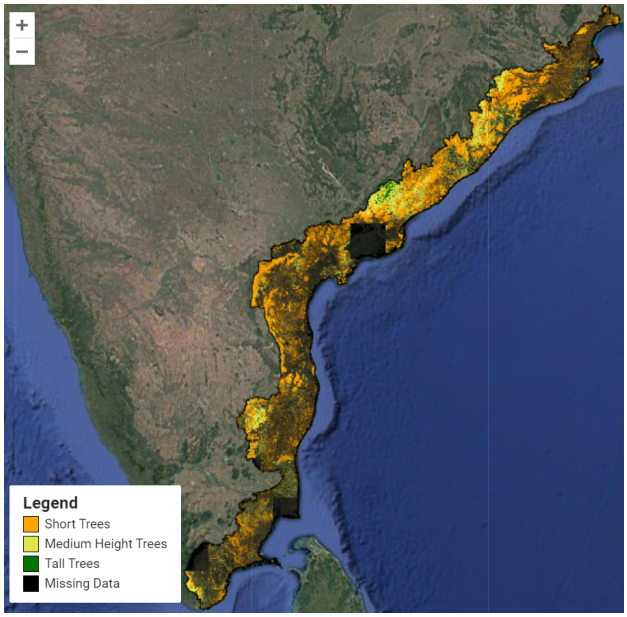
Figure 22: Tree Health Output Maps for Southern Plateau and Hills Region



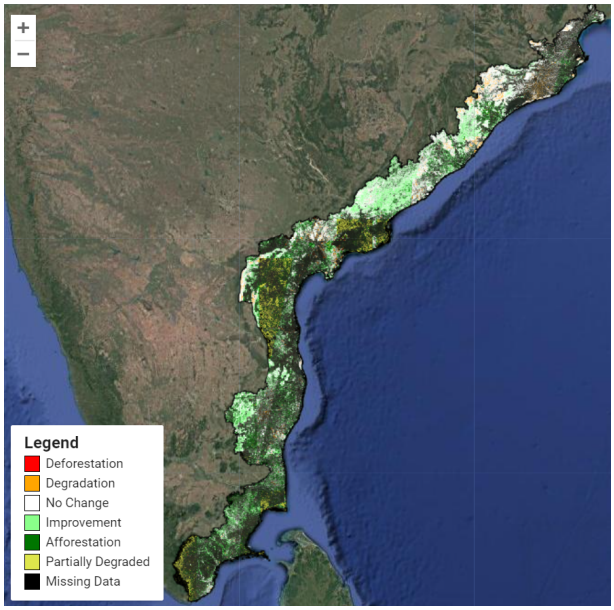
(a) Tree Cover in AY 2021



(b) CCD Outputs for AY 2021



(c) CH Outputs for AY 2021



(d) Overall Tree Health Change from AY 2017 to 2021

Figure 23: Tree Health Output Maps for East Coast Plains and Hills Region